Constant Speed Wind Farm Dynamic Model Validation

Alsvik measurements and simulations

J.T.G. Pierik T.G. van Engelen

ABSTRACT

In this report the Constant Speed Stall (CSS) wind farm dynamic model of the Erao-2 project is validated. Simulation results are compared to measurements of the Alsvik wind farm, located on the island of Gotland. Three types of measurements have been used: 62.5 Hz mechanical and electrical measurements, 256 Hz electrical measurements under normal operation and 256 Hz electrical measurements during a dip in the grid voltage. For the first two sets the Auto Power Spectral Density functions (APSDs) of measurement and simulation have been compared. For the voltage dip, the time series of the phase current, active and reactive power are compared simulations.

The validation of the model of the Alsvik wind farm showed that:

- the frequency response results of the electrical variables are good if the measured voltage is used as input instead of using a grid model;
- the frequency response results of mechanical variables are less good, which may partly
 be caused by variation of the grid voltage, which could not be used as input because it
 was not measured;
- the results for the voltage dip were quite good, with some mismatch in the damping.

The use of a closed loop measurement, viz. the measured voltage, as input for the simulations is discussed. It is demonstrated that this introduces an error but also that the error is small for the Alsvik case.

This report is the second of a set of three reports that documents the results of the project "Verificatie dynamische modellen van windparken (Erao-3)". The other two reports are entitled:

- Validation of dynamic models of wind farms (Erao-3): Executive summay, benchmark results and model improvements [6];
- Variable Speed Wind Turbine Dynamic Model Validation: JWT measurements and simulations [7].

Keywords: wind turbine models, wind farm models, model validation, wind farm dynamics, wind farm electrical systems

Acknowledgement

Erao-3 is a continuation of the Erao projects on the development of steady state (load flow) and economic models (Erao-1) and dynamic models of offshore wind farms (Erao-2). The Erao projects have been supported by the Dutch Agency for Energy and Environment (NOVEM) in the "Programma Duurzame Energie" of the Netherlands, executed by Novem by order of the Ministry of Economic Affairs.

The measurement data of the Alsvik wind farm have been supplied by Chalmers University of Technology in the framework of the IEA Annex XXI: Dynamic models of Wind Farms for Power System studies.

Novem project number: 2020-02-12-10-002

ECN project number: 7.4336

Constant Speed Wind Farm Dynamic Model Validation			
•			

CONTENTS

1	Introduction		7
2	Alsv	ik wind farm model validation method	9
	2.1	Simulation of a rotor effective wind speed and terminal voltage	9
3	Alsv	ik turbine and wind farm data	11
	3.1	Alsvik turbine data	11
	3.2	Alsvik electrical parameters	14
4	Alsv	rik wind farm model	15
5	Alsv	ik measurements	21
	5.1	Wind speed calculation	21
6	Alsv	rik wind farm model validation	23
	6.1	Validation 1 - measurement set 1 : Alsvik normal operation, 62.5, 31.25 and 2 Hz sample frequency	23
	6.2	IEA Annex XXI benchmark case: measurement WD285WS100-1	27
	6.3	Validation 2 - measurement set 3 : Alsvik normal operation, 256 Hz sample frequency, voltage from grid model	29
	6.4	Validation 3 - measurement set 3 : Alsvik normal operation, 256 Hz sample frequency, measured voltage input	33
	6.5	Validation 4 - measurement 4: Alsvik Turbine 3 voltage dip	39
7	Con	clusions	46
A	Vali	dation of models using a closed loop measurement as input	50
	A.1	System identification theory approach	51
	A.2	Estimation of the correlation between wind speed and voltage	55
	A.3	Summary of parameters in random processes	61
	A.4	Cross and auto power spectral relation	63
В	Alsv	ik windfarm parameters	64

ECN-E-07-007 5

Constant Speed Wind Farm Dynamic Model Validation		

1 INTRODUCTION

In the Netherlands the first steps towards large scale implementation of offshore wind power have been taken. The first offshore wind farm of about 100 MW, located near the coast of Egmond in the province of North Holland has been built. Plans exist for a substancial amount of offshore wind energy in the Dutch section of the North Sea. These offshore wind farm will feed into the Dutch high voltage grid. The effect of large amounts of wind power on the grid are not that well known yet. Only the steady state behaviour has been considered thus far, resulting in suggestions for grid reinforcement. The investigation needs to be complemented with a study on the dynamic interaction of wind power and high voltage grid.

A crucial aspect of large scale implementation of wind energy will be the effect on grid stability and reliability of electricity supply. Secondly, the effect of wind power on the amount of rotating reserve and back-up power is of economic importance.

Wind turbine and wind farm control can play a role in grid control and thereby increase the value of wind power. Currently, there is relatively little experience with large wind farms and their effect on grid control. The models to evaluate these effects, locally as well as on the level of a grid control area, are now becoming available.

Dynamic models of wind farms have been developed by a number of research institutes in Europe and America. ECN and TUD have developed steady state and dynamic models of wind farms in the Erao-1 and Erao-2 project [5, 8, 9]. The dynamic models, in combination with grid models, can be used to study a number of dynamic phenomena, viz. voltage and frequency transients, small signal stability, effect of wind power on rotating reserve, wind farm and grid response during short circuits and other extreme events etc. These studies can improve wind turbine, wind farm and grid control.

A group of nine research institues has started the IEA Annex XXI: *Dynamic models of Wind Farms for Power System studies* to validate dynamic models [11]. The overall objective of the IEA Annex 21 is to develop and validate models of wind turbines and wind farms. The emphasis is on models suitable for evaluating power system dynamic and transient stability. The Annex comprises the following objectives:

- Establishment of an international forum for exchanging knowledge and experience within the field of wind farm modelling for power system studies;
- Development, description and validation of wind farm models. The wind farm models are developed by the individual participants of the Annex, while the description and validation will be coordinated by the Annex as to give the state of the art and to pinpoint key issues for further development;
- Set-up and operation of a common database for benchmark testing of wind turbine and wind farm models as an aid for securing good quality models.

In the Netherlands the Erao-3 project was executed by ECN and TUD with financial support of Novem. The objective of this project is the validation of dynamic models of wind farms within the framework of the IEA Annex XXI. The Erao-3 project includes the following activities:

- Validation of two types of dynamic models of wind farms: Constant Speed Stall (CSS) and Variable Speed Pitch (VSP);
- Improvement of the wind turbine and wind farm models;

ECN-E-07-007

- Search for available measurements of Dutch wind farms for incorporation in the IEA database;
- Participation in the IEA Annex XXI meetings;
- Reporting of activities and results.

This report covers part of the activities and results of the Erao-3 project, viz. the verification of the Constant Speed Stall wind farm model (CSS Wind Farm). This report is the second of a set of three reports that documents the results of the project "Verificatie dynamische modellen van windparken (Erao-3)". The other two reports are titled:

- Validation of dynamic models of wind farms (Erao-3): Executive summay, benchmark results and model improvements [6];
- Variable Speed Wind Turbine Dynamic Model Validation: JWT measurements and simulations [7].

The Alsvik wind farm measurements are part of the IEA Annex XXI data base and have been chosen for the first validation of the CSS wind turbine and wind fam model for the following reasons:

- measurement data of four constant speed turbines is available;
- the measurements have been recorded at relatively high sample rates (31.25, 62.5 and 256 Hz, depending on the type of measurement);
- measurements are available for a range of conditions (different wind speeds and wind directions and different operating conditions: normal operation as well as operation during a voltage dip at the terminals of the generator);
- the turbine and farm parameters are available and relatively well known.

2 ALSVIK WIND FARM MODEL VALIDATION METHOD

The dynamic model of the Alsvik constant speed wind farm will be validated by comparing simulations to the Alsvik wind farm measurements. The validation will for the most part compare the frequency content of the simulations to the frequency content in the measurements. Directly comparing time series of individual signals is problematic, as will be discussed in section 2.1.

Prior to the simulation of the wind farm, the following steps have been taken:

- Investigation of the available Alsvik measurements;
- Choice of measurements to be simulated;
- Preparation of a complete list of input parameters required for the Alsvik dynamic wind farm model;
- Preparation of the Alsvik wind farm model using the component models in the Erao-2 model library;
- Calculation of a rotor effective wind speed time series for each of the turbines in the farm:
- Simulation of the wind turbine terminal voltage (if the voltage is not measured or if direct use causes a too large bias in the calculated frequency response).

2.1 Simulation of a rotor effective wind speed and terminal voltage

The measured instantaneous single point wind speed is not a good dynamic representation of the instantaneous rotor effective wind speed at each of the four turbines during the measurements. This is caused by the distance between the meteo mast and the turbine, the variation of the wind speed over the rotor plane and the rotational sampling by the rotor. The rotor effective wind speed is difficult to measure, maybe the turbine itself is the best measuring device, but a model would be required to reproduce the rotor effective wind speed. The accuracy of this model would compromise this model validation or make validation impossible by intoducing a vicious circle.

For the simulation of the dynamic behaviour of the wind turbine, the unavailability of an accurate instantaneous value of the rotor effective wind speed is a problem. The instantaneous values of simulated variables like turbine power etc. will not match the corresponding instantaneous measured values and validation by comparing time series is practically impossible.

Statistically, the rotor effective wind speed is well known however. This fact can be used to construct a statistically correct time series of the rotor effective wind for a given turbine type based on the average wind speed in the measurement. The method is described in ECN-reports [14] and in [15]. As long as only the dynamic changes in voltage, current, power and other turbine variables are compared, i.e. the frequency response of a model is validated, the exact instantaneous value of the rotor effective wind speed during the measurement is not needed. To validate the frequency response, the Auto Power Spectral Density functions (APSDs) of simulation and measurement will be compared. The major drawback of this method is that a high measurement sample frequency and proper signal conditioning (anti-aliasing filters) are required, in order to prepare correct APSDs with a sufficiently high cut-off frequency.

A second issue to be investiged before the validation can be executed, is which source should be used for the second model input variable: the wind turbine terminal voltage. At first glance,

ECN-E-07-007

it seems obvious to use the measured terminal voltage, if available. There is a problem with this choice however, if the frequency response of the model is compared to the frequency content of the measurement. The voltage is not an independent variable: for a constant speed turbine it may strongly depend on the rotor effective wind speed. System identification theory shows that this makes it impossible to determine the transfer function of the turbine between voltage and current or power, see appendix A. Secondly, the correlation between wind speed and current will lead to an error or bias in the simulatated dynamic behavour and the resulting APSDs. Appendix A gives the analytical background of this problem and also a quantification for the Alsvik wind farm case. It is shown that for the Alsvik wind farm the error in the frequency response caused by using the measured voltage as an input is small because the coherence between the rotor effective wind speed and the voltage is expected to be small due to two circumstances:

- multiple turbines in operation;
- a substantial amount of noise on the voltage signal caused by load changes deeper in the grid.

A different approach is to use a grid model to generate the wind turbine terminal voltages or to assume that the voltage is constant (infinitely strong grid). If no voltage measurement is available, this is the only option. The effect of using a grid model instead of a measured voltage will be investigated in chapter 6.

3 ALSVIK TURBINE AND WIND FARM DATA

The Alsvik wind farm consists of four Danwin 180 kW constant speed turbines. The farm is located close to the Baltic Sea on the island of Gotland. The location of the turbines and the meteo mast are shown in figure 1.

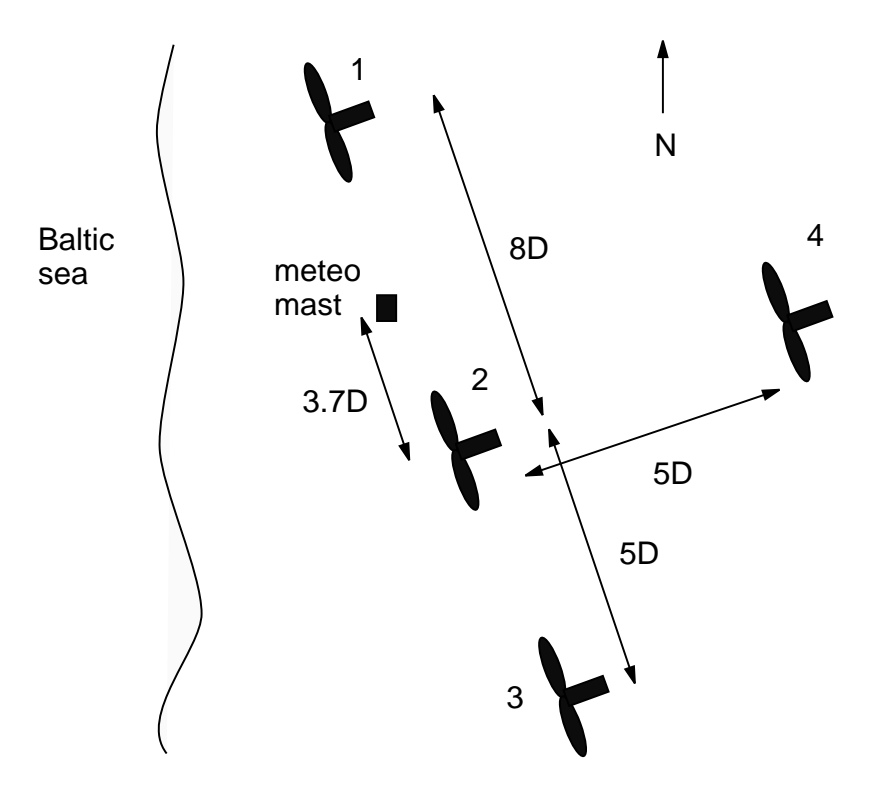


Figure 1: Layout of Alsvik wind farm

3.1 Alsvik turbine data

The turbine and farm parameters have been supplied by Chalmers [12, 13] and Teknikgruppen [1] and have been supplemented by ECN calculations.

The C_p and C_{dax} values are essential and three different sources were available: measurements (but not for the full operating range) and two sets of calculations: ECN-GS¹ and ECN-EB². The calculations use the blade data (C_L and C_D per blade section). The difference between the two calculations are caused by minor differences in the blade geometry, viz. how the blade is divided into sections, and the use of a different computer model. The calculated results are compared to Alsvik turbine measurements.

The electric power in table 1 has been measured by FFA at the Alsvik turbine [2]. The aero-dynamic power in this table and the axial force coefficients in table 2 have been calculated by ECN [10].

ECN-E-07-007

¹Phatas evaluation by G. Schepers (ECN)

²ATG (Aerodynamic Table Generator) evaluation by E. Bot (ECN)

Table 1: Measured electric and calculated aerodynamic power of the Alsvik Danwin 180 kW turbine

wind speed	electric power	aero power
m/s	W	W
4.8	9.13e3	12.53e3
5.61	15.85e3	20.30e3
6.52	29.59e3	35.9e3
7.51	50.83e3	59.8e3
8.48	73.03e3	85.9e3
9.46	97.97e3	115.3e3
10.47	123.0e3	144.7e3
11.43	144.6e3	170.11e3
12.43	163.0e3	191.8e3
13.45	175.0e3	208.3e3
14.45	175.0e3	208.3e3
15.37	164.0e3	192.94e3
16.15	147.0e3	172.94e3

Table 2: Calculated axial force coefficients of the Alsvik Danwin 180 kW turbine [10]

wind speed	ax. force coeff.
m/s	(-)
3.999	1.110
4.159	1.098
4.333	1.084
4.521	1.065
4.726	1.045
4.952	1.025
5.199	1.007
5.473	0.988
5.777	0.967
6.117	0.945
6.499	0.921
6.932	0.895
7.427	0.864
7.999	0.829
8.665	0.791
9.453	0.748
10.398	0.695
11.554	0.619
12.998	0.527
14.855	0.431
15.997	0.371
17.330	0.309

The calculated values are used to extend the range of the measured values. Figure 2 and 3 compare measurements to calculations. The ECN-EB values show deviations in C_t for low wind speed (C_t is a few percent too low) and in P for high wind speed (above 15 m/s the calculated value is too high, above 17 m/s no measurement is available). The ECN-GS power values practically coincide with the measurements, while the C_t is 10% too high at low wind speed. The ECN-GS parameter values will be used for the validation.

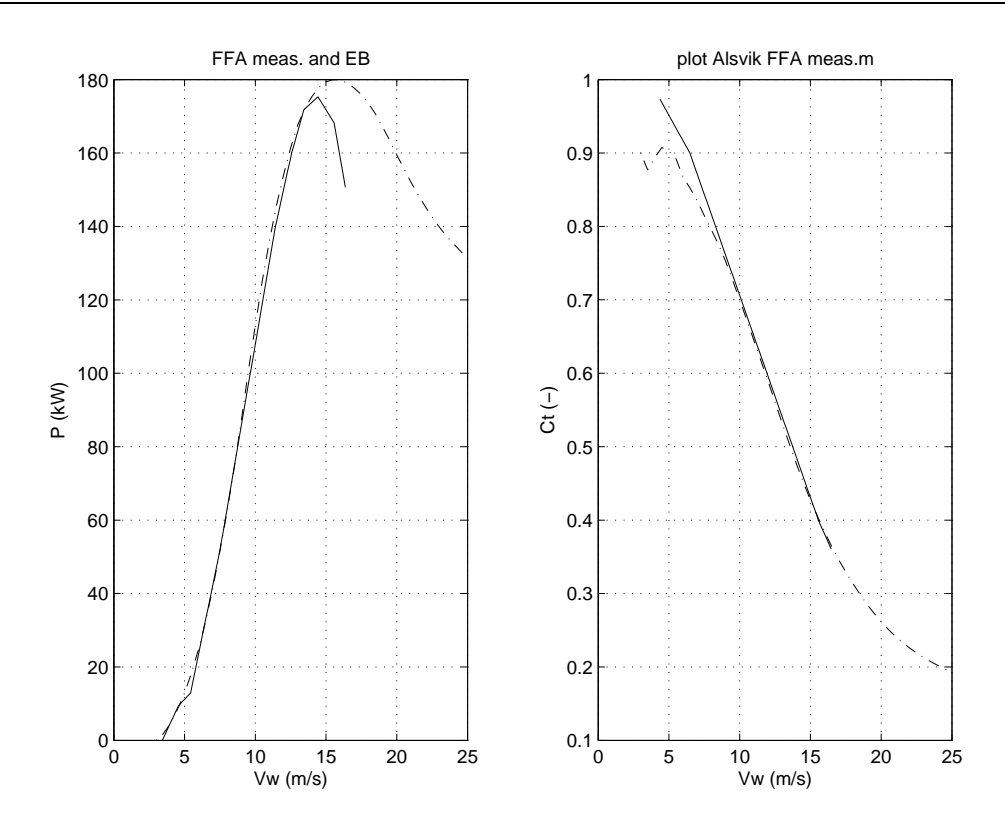


Figure 2: Alsvik: FFA measurements [2] (solid line) versus ECN-EB calculation

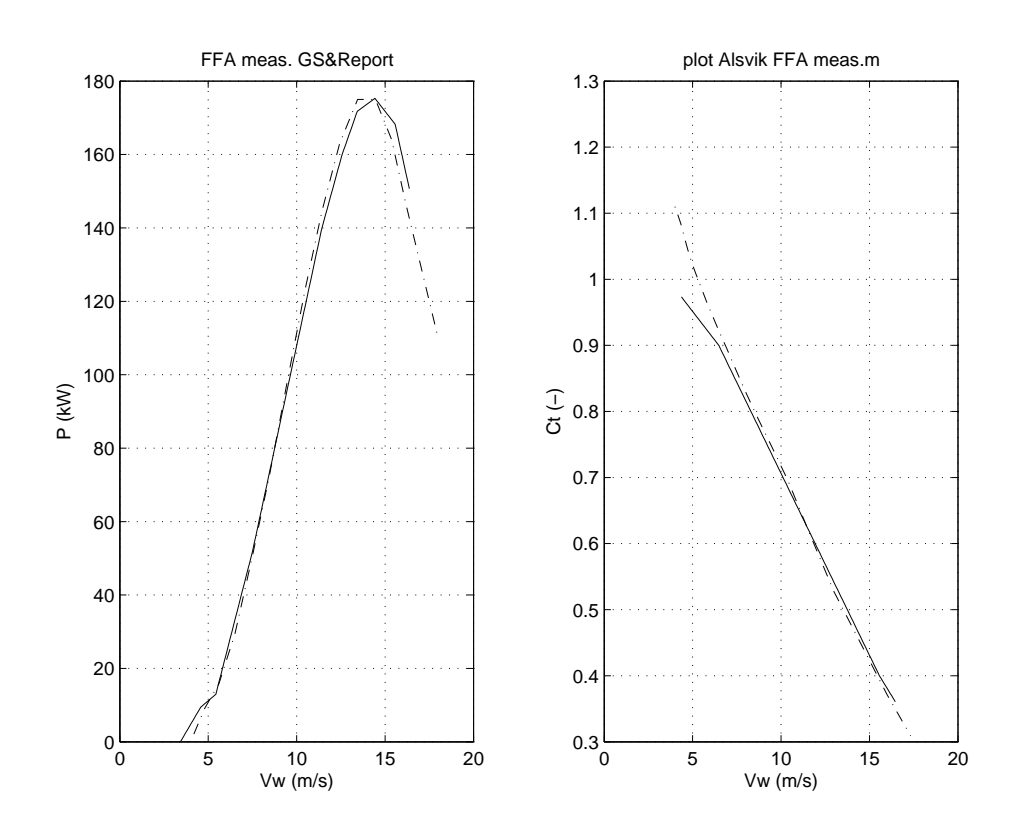


Figure 3: Alsvik: FFA measurements [2] (solid line) versus ECN-GS calculation

3.2 Alsvik electrical parameters

The parameters of the electrical components in the Alsvik wind farm model are listed in table 3.

Table 3: Electrical parameters of Alsvik Danwin 180 kW turbine

Generator		
Type	Asynchronous	
Voltage	415 V	
Frequency	50 Hz	
Nr. of pole pairs	3	
R_s	0.0092Ω	
R_r	$0.0061~\Omega$	
L_m	6.7 mH	
L_{sl}	0.186 mH	
L_{rl}	0.427 mH	
Turbine transformer plus turbine cable		
R_p	0.0076Ω	
X_p	$0.0209~\Omega$	
Grid transformer plus grid cable		
R_g	6.5 Ω	
X_g	7.1 Ω	

4 ALSVIK WIND FARM MODEL

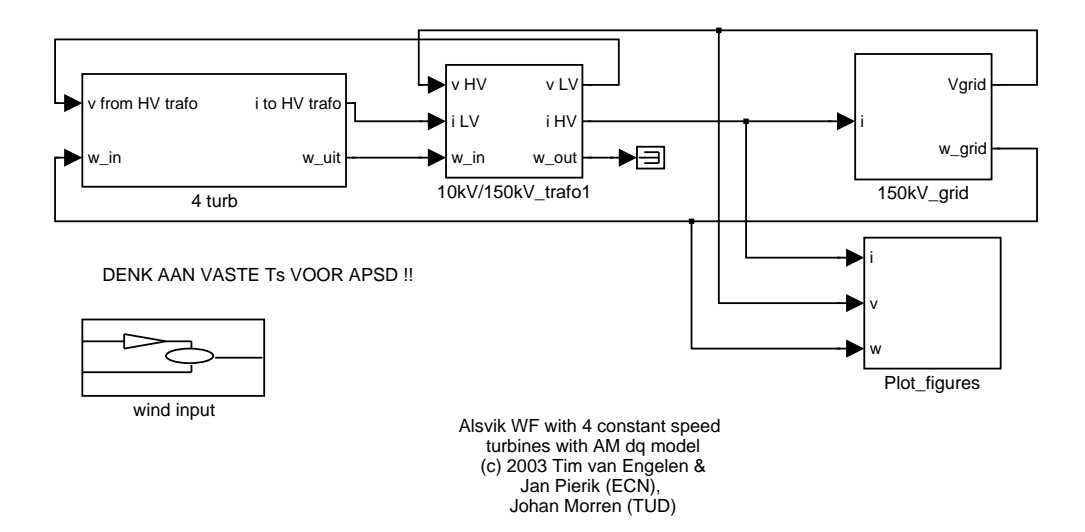


Figure 4: Erao Simulink model of Alsvik Wind Farm

The constant speed stall wind farm model validated in this report has been developed by ECN and TUD in the Erao-2 project [8]. The dynamic model is programmed in Simulink, a simulation language for dynamic modelling and controller design. The normalised rotor effective wind speed is generated by a separate model, writen in Matlab. The Simulink model of the Alsvik wind farm will be illustrated by a few Simulink model diagrams, which show the submodels and the signal flow. For the mathematical formulas of the CSS wind turbine model and the electrical models, as well as the grid model, is referred to [8], also available at the web site of ECN (www.ecn.nl, use search option). The Simulink model (see figure 4) consists of three main parts:

- the Alsvik wind farm model;
- the 10/150 kV transformer model;
- the grid model.

The model of the Alsvik wind farm (see figure 5) includes models of:

- four constant speed stall controlled turbines;
- four 10 kV cables connecting the turbines to a 10-150 V transformer.

The model of the constant speed stall controlled turbine (see figure 6) includes:

- the turbine transformer;
- the constant speed stall (CSS) model for the Alsvik turbine.

The Alsvik constant speed stall model (see figure 7) includes:

• the fourth order dq-model of an asynchronous generator (see figure 8);

ECN-E-07-007

- the rotor effective wind calculation including turbulence, wind shear and tower passage (see figure 9);
- the rotor model based on tables of aerodynamic coefficients C_p , C_q and C_t (see figure 10):
- the mechanical model of the turbine.

The mechanical model of the turbine includes (see figure 11):

- a two masses-spring-damper model of drive train;
- a single mass-spring-damper model of tower and nacelle (tower motion in two directions: nodding and naying).

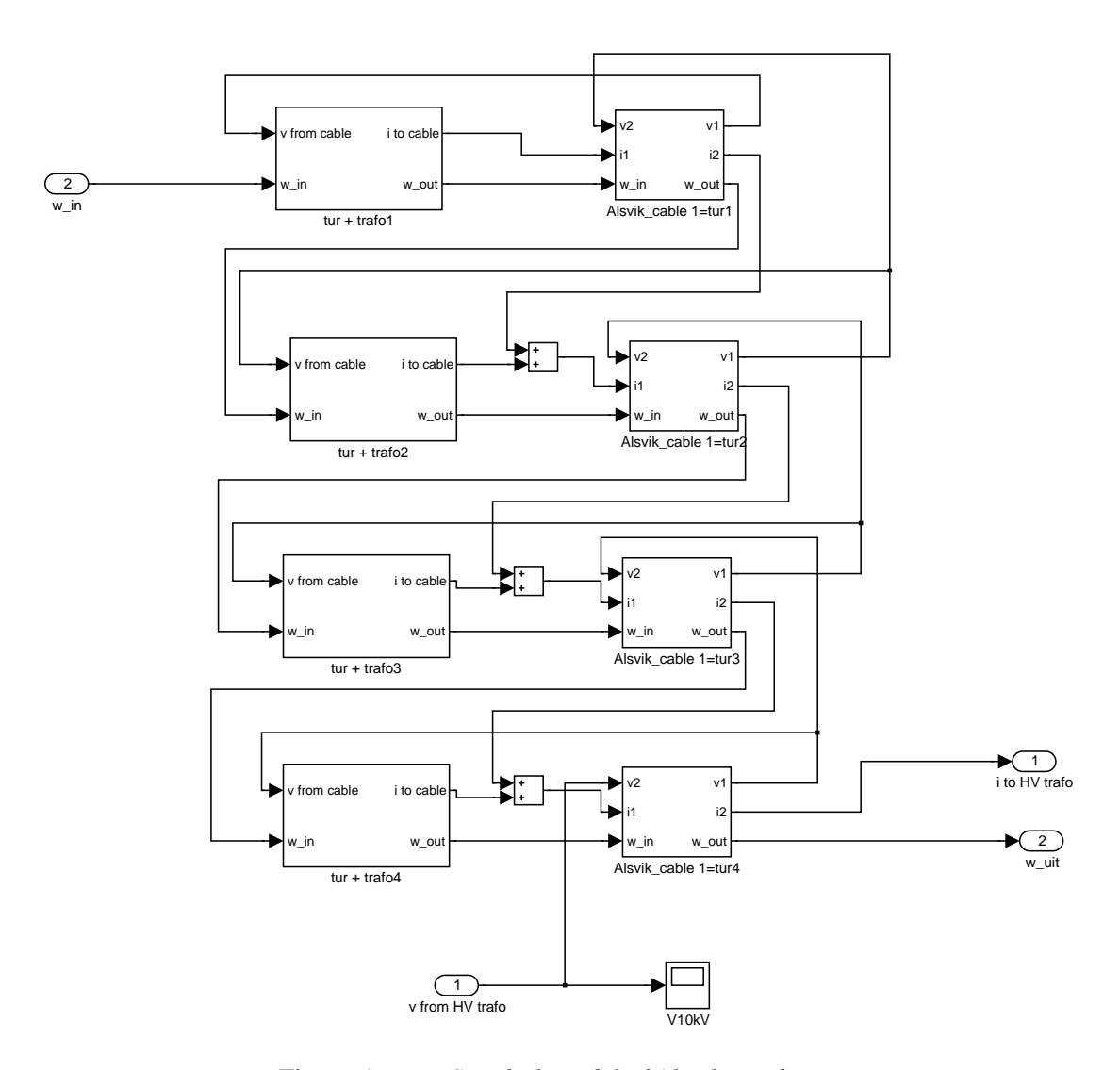


Figure 5: Erao Simulink model of Alsvik Wind Farm

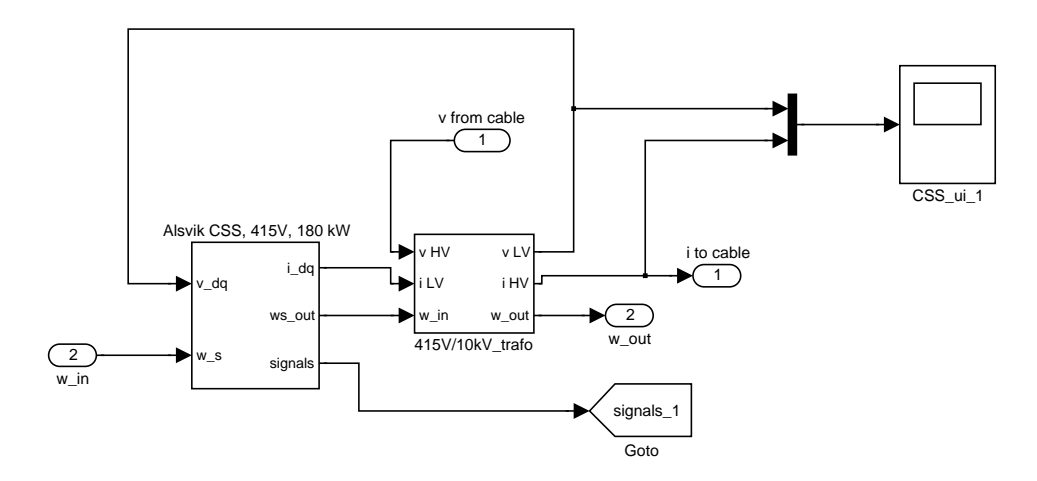


Figure 6: Erao Simulink model of Alsvik Turbine and transformer

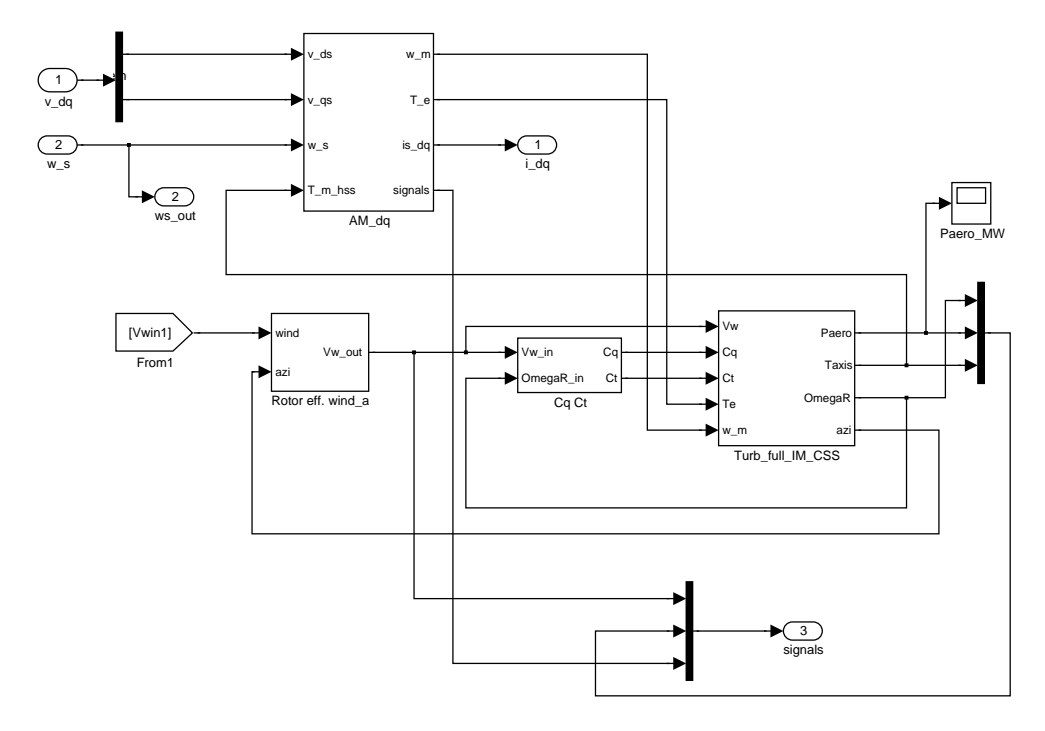


Figure 7: Erao Simulink model of Alsvik Turbine

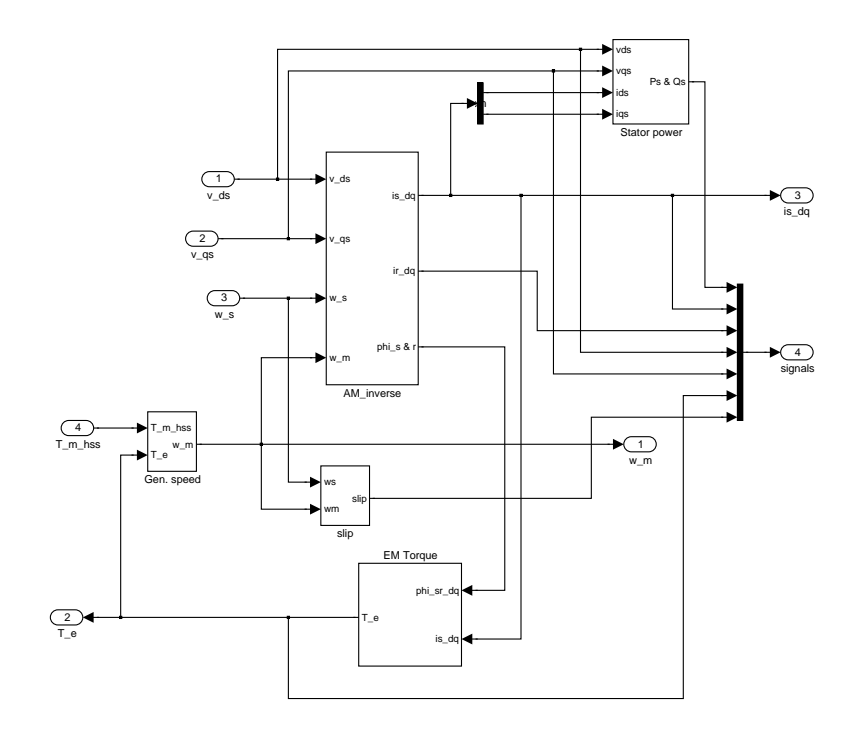


Figure 8: Alsvik Turbine generator model

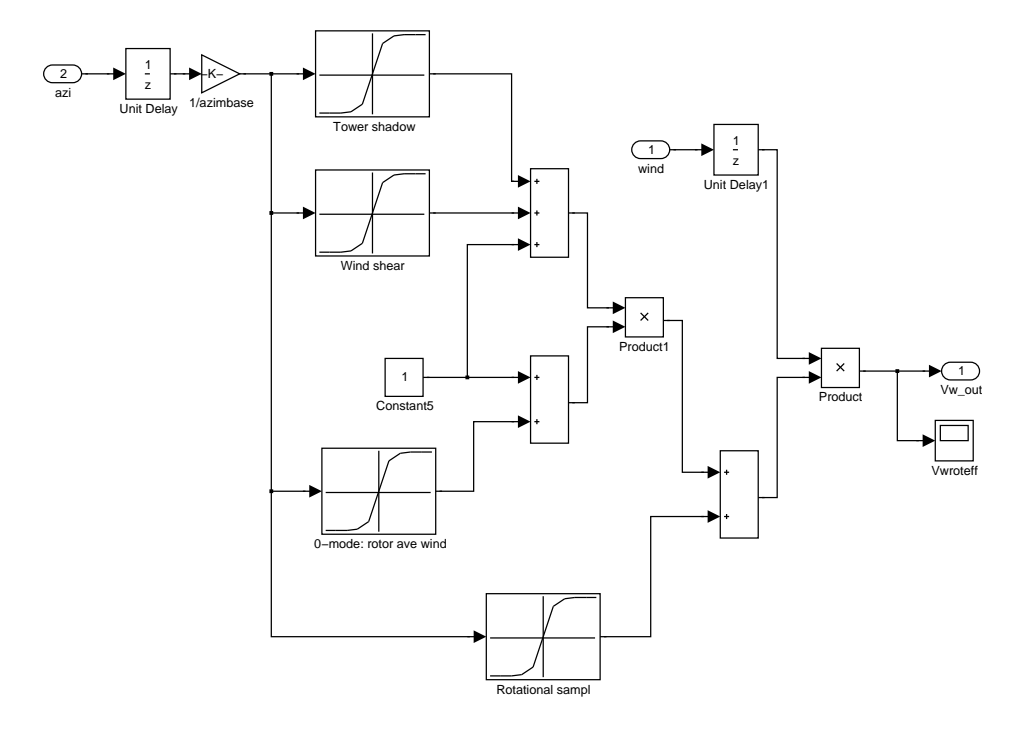


Figure 9: Alsvik Turbine rotor effective wind speed model

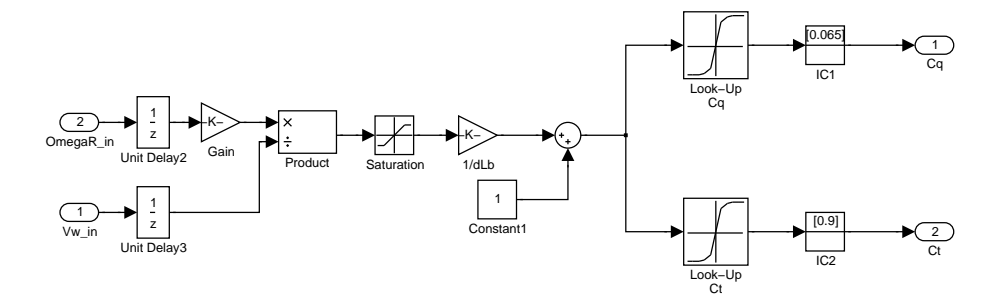


Figure 10: Alsvik Turbine aerodynamic model

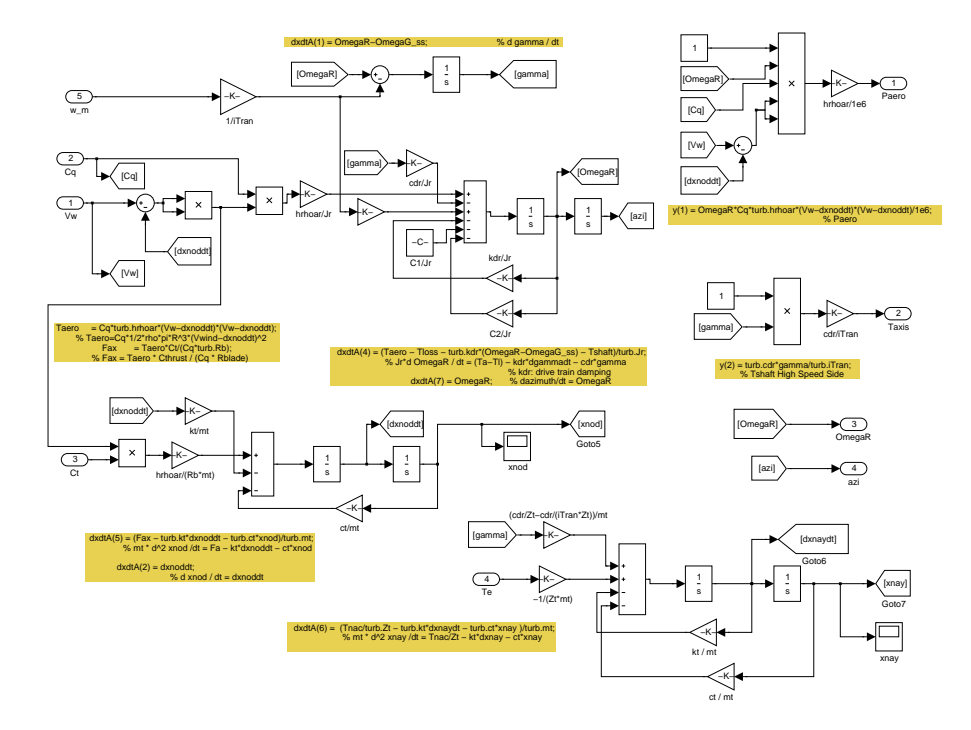


Figure 11: Alsvik Turbine mechanical model

In some of the simulations a grid model is included (see figure 12), which includes models of the following components:

- a 10-150 kV transfomer;
- a 150 kV cable;
- a 150-13.8kV transfomer;
- a 13.8 kV cable;
- two consumer loads (resistors);
- a voltage and frequency controlled synchronous generator (fifth order dynamic model).

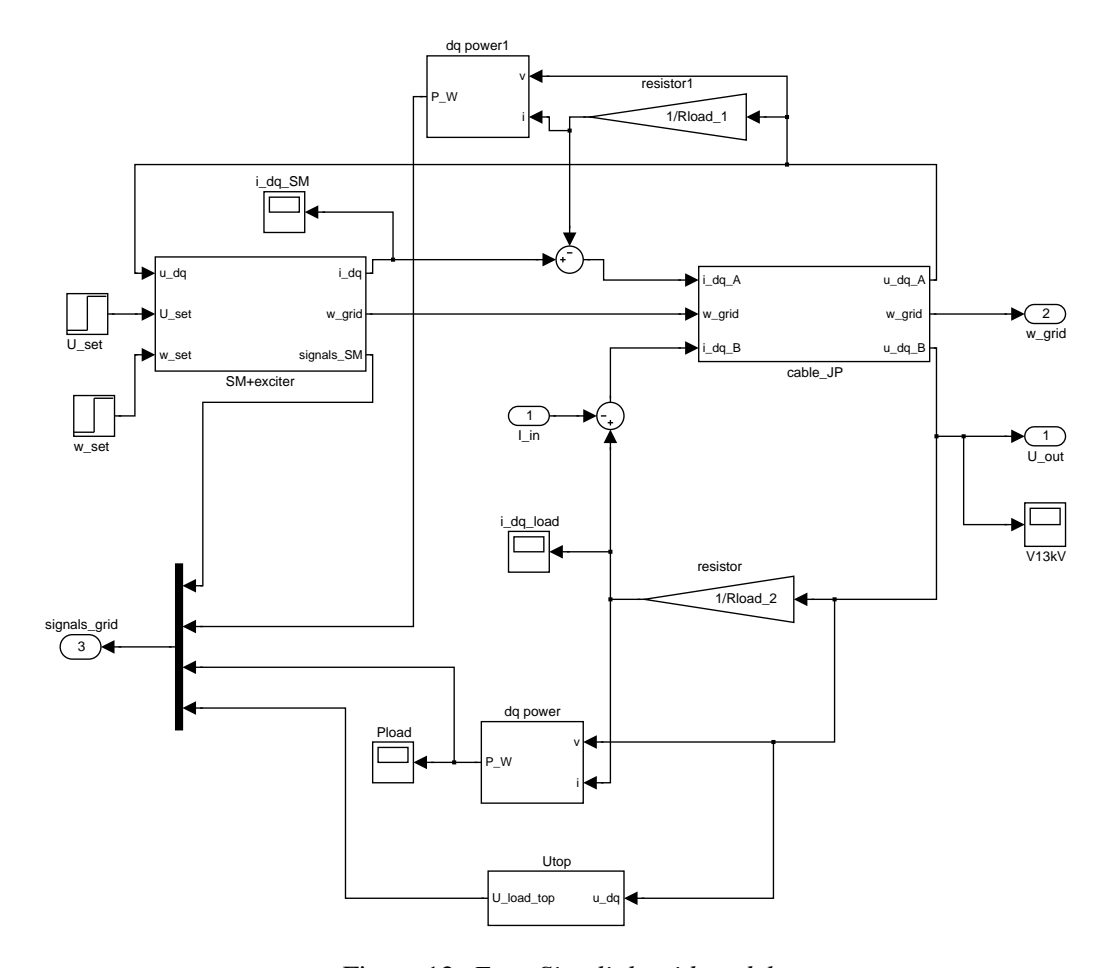


Figure 12: Erao Simulink grid model

The component parameters of the Alsvik wind farm model are listed in appendix B tables 10, 11 and 12.

5 ALSVIK MEASUREMENTS

The Alsvik measurements comprise three types of measurement:

- 1. *Measurement set 1 and 2*: mechanical and electrical variables of turbine 4, recorded at rates of 62.5, 31.25 and 2 Hz. The wind farm is operating under normal conditions at different wind speeds and directions;
- 2. *Measurement set 3*: electrical variables of turbines 2, 3 and 4, recorded at a rate of 256 Hz. The wind farm is operating under normal conditions at different wind speeds and directions;
- 3. *Measurement set 4*: electrical variables of turbines 3, recorded at a rate of 256 Hz. The wind turbine operation is abnormal: a voltage dip.

The measurement have been performed by the Department of Electric Power Engineering of Chalmers University of Technology, Goteborg, Sweden and contributed to the IEA Annex XXI database.

5.1 Wind speed calculation

The wind speed has been measured at mast 1, located between turbine 1 and 2. Wind speed and wind direction at hub height is available at 31.5 Hz sample rate. Additionally wind speed at hub height and at bottom and top of rotor disc measured at 2 Hz are available. The wind speed measurements are single point wind speeds, as opposed to the wind speed seen by a turbine rotor, i.e. rotor effective wind speed.

The rotor effective wind speed is required for realistic simulation of the individual turbines in the farm. As discussed in section 2.1, the validation will use a statistically correct realisation of the rotor effective wind speed generated by a wind speed model and based on the average wind speed and turbulence of the single point wind speed in the measurements. The validation based on measurement set 1, 2 and 3 will not compare time series but instead will compare the frequency content of simulation and measurement. For each of the turbines in the farm a scaled realisation of the rotor effective wind speed is generated prior to the simulation. The properties of the turbine rotor and the blade position (the azimuth angle) are taken into account in the wind speed calculation. The resulting rotor effective wind speed consists of four components:

- the 0P component, representing the uniform wind speed variations averaged over the whole rotor plane;
- the 3P and 6P variations, representing rotational sampling of differences of wind speed in the rotor plane as seen by a blade rotating with P revolutions per second;
- the wind shear sampled by the turbine blades;
- the tower shadow sampled by the blades.

Figure 13 compares the single point and the rotor effective wind speed spectra. The single point measurement frequency content is higher in some frequency ranges and does not include the nP peaks.

During some of the measurements, the meteo mast or a turbine is in the wake of another turbine. This may require a correction on the turbulence value and the average wind speed of

ECN-E-07-007 21

the measurement. If the turbine operates in a wake, the correction can be estimated by the wind farm aerodynamic and fatigue program FindFarm (offline calculation) or by the GCL-model wind farm wake model (implemented in Simulink). If the meteo mast is in the wake, but not the turbine itself, the turbulence level of a different measurement, in which this problem does not occur, is used.

Since the wind farm consists of four turbines, four different rotor effective wind speed time series are needed. To ensure that the rotor positions of the four turbines do not synchronise, different initial values of the azimuth angle are chosen.

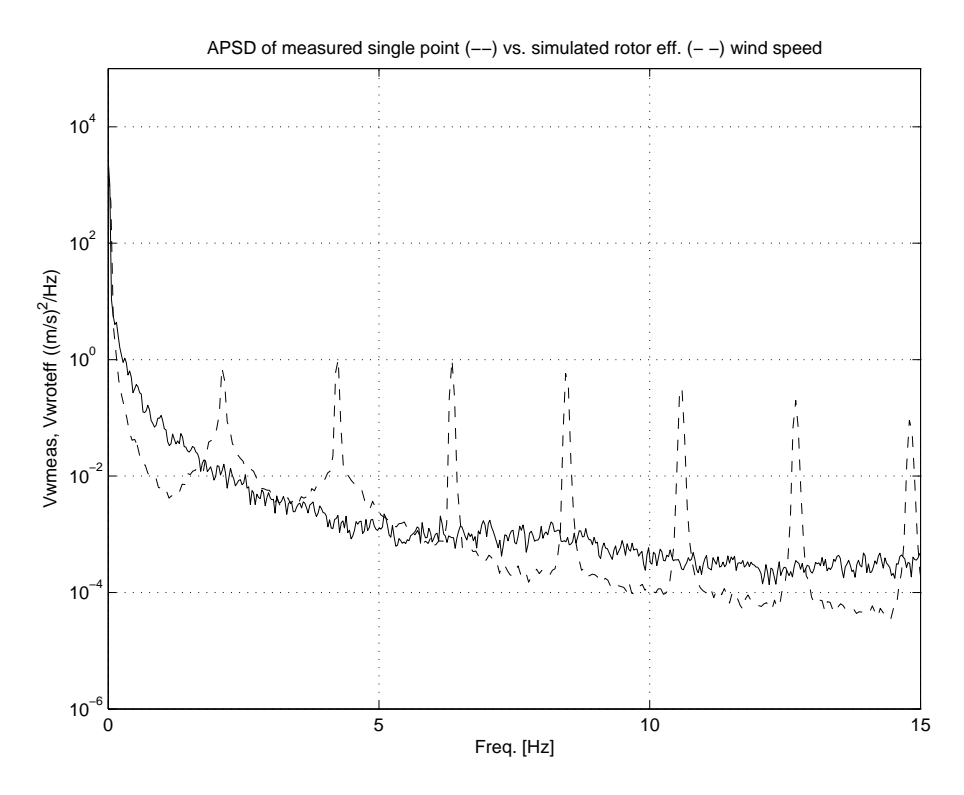


Figure 13: Measured single point wind speed (WD008WS100-2) and simulated rotor effective wind speed APSD ($I_{15class}=0.055$)

6 ALSVIK WIND FARM MODEL VALIDATION

6.1 Validation 1 - measurement set 1 : Alsvik normal operation, 62.5, 31.25 and 2 Hz sample frequency

Table 4: Measurement set 1: Alsvik normal operation, 62.5, 31.25 and 2 Hz sample frequency

Turbine 4, Sampling speed 62.5 Hz:		
ACC1	Accelerometer signal in nacelle direction	
ACC2	Accelerometer signal in edgewise direction	
ACC3	Accelerometer signal in torsional direction	
Pkort	Active power, high bandwidth (kW)	
Pkortbinary	Active power, high bandwidth (special scaling)	
Qkort	Reactive power, high bandwidth (kVA)	
Qkortbinary	Reactive power, high bandwidth (special scaling)	
edge	Shaft torque determined from blade-root signals;	
flap1	flap-directional stress in blade 1	
flap2	flap-directional stress in blade 2	
flap3	flap-directional stress in blade 3	
time1	62.5 Hz time vector (sec)	
Turbine 4, Sam	pling speed 31.25 Hz:	
T1	Tower moment in nacelle direction 6.9 m below centra	
T2	Tower moment in nacelle direction 4.9 m below centra	
T3	Tower moment in cross nacelle direction 6.9 m below centra	
T4	Tower moment in cross nacelle direction 4.9 m below centra	
T5	Torsional moment, positive in clockwise direction (seen from above)	
pow4	Power turbine 4 (2 Hz bandwidth) (kW)	
WD	Wind direction (Deg)	
WS2	Wind speed at hub height (m/s)	
NacD	Nacelle direction (deg)	
newangle	Rotor position (deg) (0 deg = blade 1 pointing upwards)	
time2	31.25 Hz time vector (sec)	
Sampling speed 2 Hz:		
Pow1slow	Power turbine 1 (2 Hz bandwidth) (kW)	
Pow2slow	Power turbine 2 (2 Hz bandwidth) (kW)	
Pow3slow	Power turbine 3 (2 Hz bandwidth) (kW)	
Pow4slow	Power turbine 4 (2 Hz bandwidth) (kW)	
WDslow	Wind direction) (Deg)	
WS1slow	Wind speed at bottom of rotor disc (m/s)	
WS2slow	Wind speed at hub height (m/s)	
WS3slow	Wind speed at top of rotor disc (m/s)	
time3	2 Hz time vector (sec)	

Table 4 lists the measured variables and the sample frequencies of measurement set 1 and 2. The $62.5 \, \text{Hz}$ and $31.25 \, \text{Hz}$ measurements have been taken at turbine 4. This has been checked by comparing Pow4slow to Pkort. This measurement does not include voltages or currents, the measurements are primarily mechanical. The mechanical model of the turbines in a model for power system studies often is relatively simple, this is also true for the Erao-2 dynamic model. Most of the mechanical variables in table 4 are not calculated in the Erao-2 turbine model, only the power, reactive power and shaft torque can be compared. Since the voltage is not measured, either a grid model can be used or the voltage can be assumed to be constant. If the measured voltage is used as an input for a simulation or if the voltage is assumed to be

ECN-E-07-007 23

constant, the electrical interaction between the turbines in the farm is not present in the model, since the voltage is not influenced by the simulated turbine outputs. In that case, including all turbines of the wind farm in the wind farm model to monitor the interaction is not an option. On the other hand, if a grid model is used, it is important to include a separate model for each turbine since the interaction will affect the results. In the first validation, the voltage is calculated by a grid model and a four turbine wind farm simulation model is used. Table 5 list the conditions of the first validation.

Table 5: Validation 1 - measurement set 1 and 2 : Alsvik normal operation, measurement and model specification (Tx = turbine number x)

Alsvik measurements validation 1	
Set 1	WD008WS100-2
	direction = 8 deg, av. wind speed = 10 m/s
Set 2 (IEA benchmark case)	WD285WS100-1
	direction = 285 deg, av. wind speed = 10 m/s
Length	600 s
Variables and sample rate	power T4, reactive power T4, mech. torque T4, wind speed T4 (62.5 Hz)
	power T1, T2, T3 and T4 (2 Hz)
Model specification	
Rotor effective wind	from model: 0P, 3P, 6P, shear and tower shadow
Turbulence level	$I_{15class} = 0.055$
Wake correction	none
Parameter deviation from Chalmers specs	none
Turbine voltage	from grid model
Grid load variation	none
Simulink model version	CSS-4-turb-Alsvik-16-Meting1.mdl
Number of turbines in wind farm model	4

The turbulence level $I_{15class}$ is defined by:

$$I_{15class} = \frac{\sigma_u \cdot (a_{class} + 1)}{Z_t + a_{class} \cdot V_{hub}} \tag{1}$$

The standard deviation calculated from the wind speed measurement WD008WS100-2 was 0.12 ($\sigma_u = 1.95$ m/s). The level may be biased due to the fact that the meteo mast is in the wake of turbine 1 in this measurement. Therefore, the turbulence level of measurement D6-F372.I32 was used (0.055).

Only turbine 4 was measured at a high sample rate. Figure 14 compares the APSD of the measured active power of turbine 4 with the APSD of the simulated active power. The levels only coincide below 1 Hz. A peak at 1.1 Hz does not appear in the simulation. Above 5 Hz the level of oscillation in the measurement is about a factor 10-100 (squared) higher and there is a broad peak at 7.5 Hz. The measurement contains a number of small peaks, which are missing in the simulation. The nP peaks in the active power are reproduced with a reasonable accuracy.

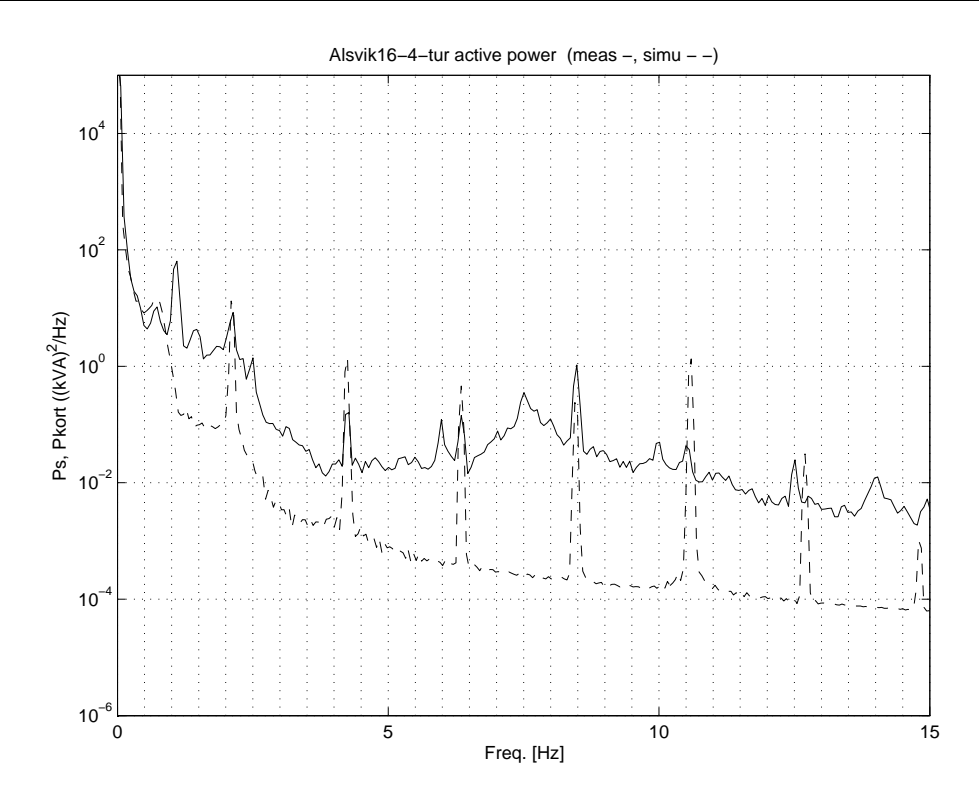


Figure 14: APSD of Measured (WD008WS100-2) and Simulated Active Power of Turbine 4

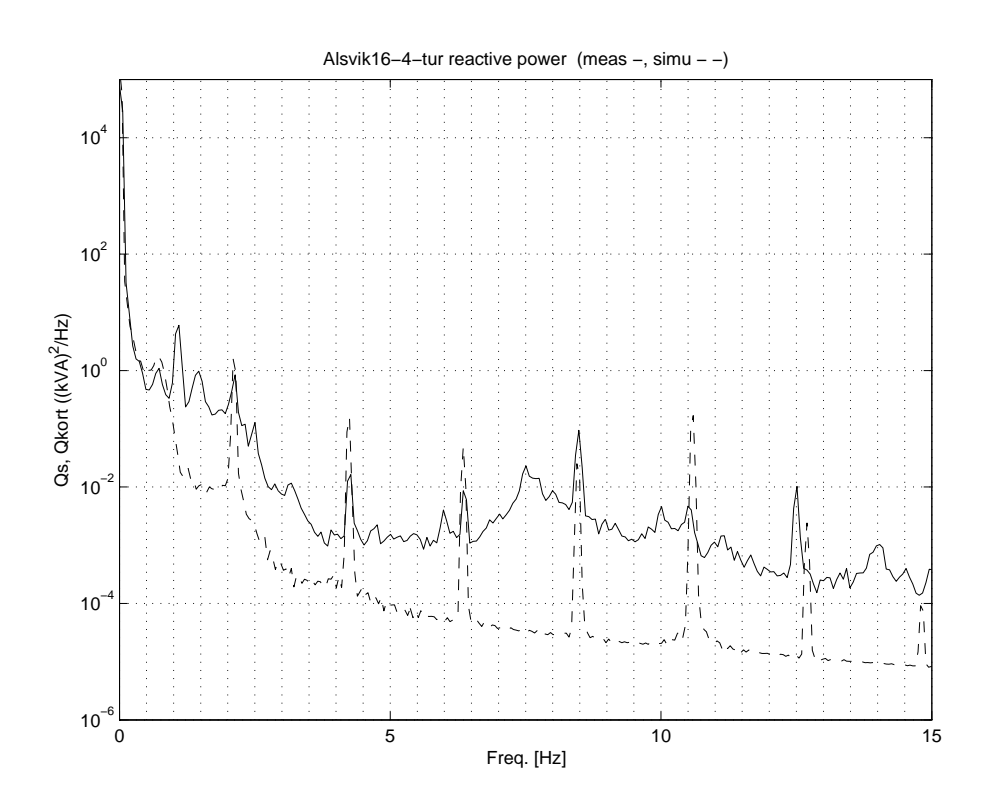


Figure 15: APSD of Measured (WD008WS100-2) and Simulated Reactive Power of Turbine 4

Figure 15 displays the APSDs of the measured and the simulated reactive power. The differences and similarties observed for the active power also appear in the reactive power.

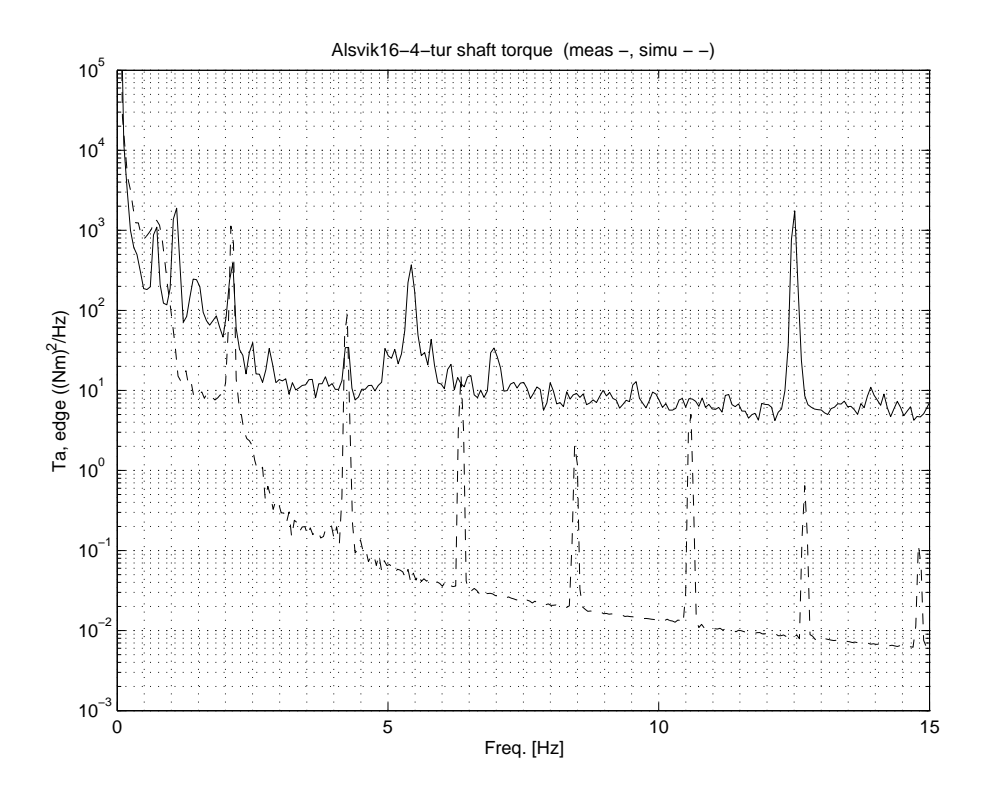


Figure 16: APSD of Measured (WD008WS100-2) and Simulated Mechanical Torque (LSS) of Turbine 4

Finally, the measured and simulated mechanical torque are compared in figure 16. The mismatch above 5 Hz is higher than for the active and reactive power (about a factor 10-1000 (squared) instead of 10-100). Severe oscillations are present in the measured torque at 5.5 and 12.5 Hz (near 6*3P). Both oscillations are missing in the simulation. The 5.5 Hz oscillation is not present in the APSD of measured active and reactive power.

Preliminary conclusion from the first validation result:

From the first comparison of measured and simulated frequency responses can be concluded that the correspondence for the Alsvik constant speed stall turbine model is not that good. Some oscillations are missing and the level of oscillation above 1 Hz is underestimated. These discrepancies can be caused by several factors:

- errors in the (mechanical) turbine parameters, for instance the parameters of the tower are not well known;
- incomplete modeling of the the turbine rotor: only a simple steady state representation of the rotor is used, blade lead-lag and flap oscillations are absent in the simulation;
- an insufficient level of detail of the electrical models (no saturation, simplified transformer and cable representations);
- an inadequate representation of the grid by a single synchonous generator and without any autonomous dynamic disturbance (no electic load changes, the only source of disturbance in the simulations is the wind acting on the turbines).

Especially the effect of the simplified rotor model and the grid model may be important. The grid model is an arbitrary model with parameters and properties, not backed in any way by

information on the grid behaviour at the Alsvik wind farm. The autonomous variation of the grid voltage (caused by the switching of electrical appliances) is not present in the grid model. Therefore, the voltage in the simulation is much less variable than in the measurement.

Alsvik measurement set 3 includes high sample rate measurements of the phase voltages. Using these measured voltage as a model input is expected to improve the results. Using the measured voltage as an input is discussed in appendix A and is further investigated in section 6.4.

6.2 IEA Annex XXI benchmark case: measurement WD285WS100-1

The IEA Annex XXI participants suggested to use measurement WD285WS100-1 as a benchmark. This is a measurement with an average wind speed of 10 m/s, so the same rotor effective wind speed can be used as in the previous case (section 6.1) and the measurement can be compared to the same simulation results. For the model specification see table 5. Figures 17 to 19 compare the APSDs of simulation and measurement WD285WS100-1. There are some differences between the APSDs of measurement WD285WS100-1 and WD008WS100-2, but the conclusions with regard to the simulated results remain the same (see section 6.1).

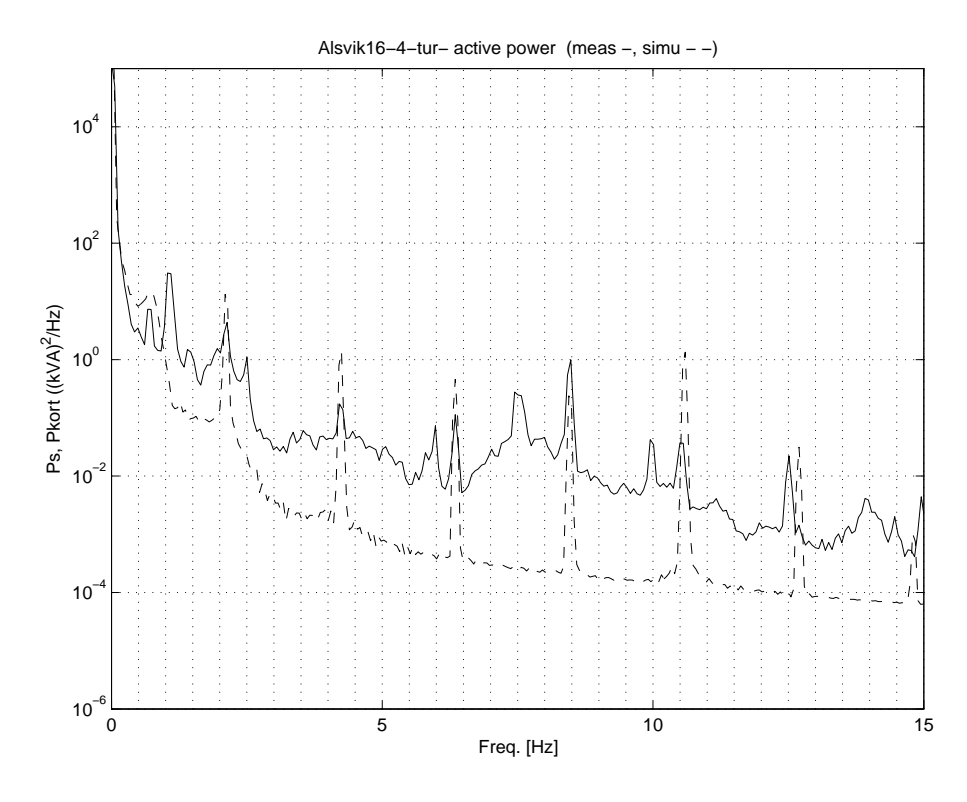


Figure 17: APSD of Measured (WD285WS100-1) and Simulated Power of Turbine 4

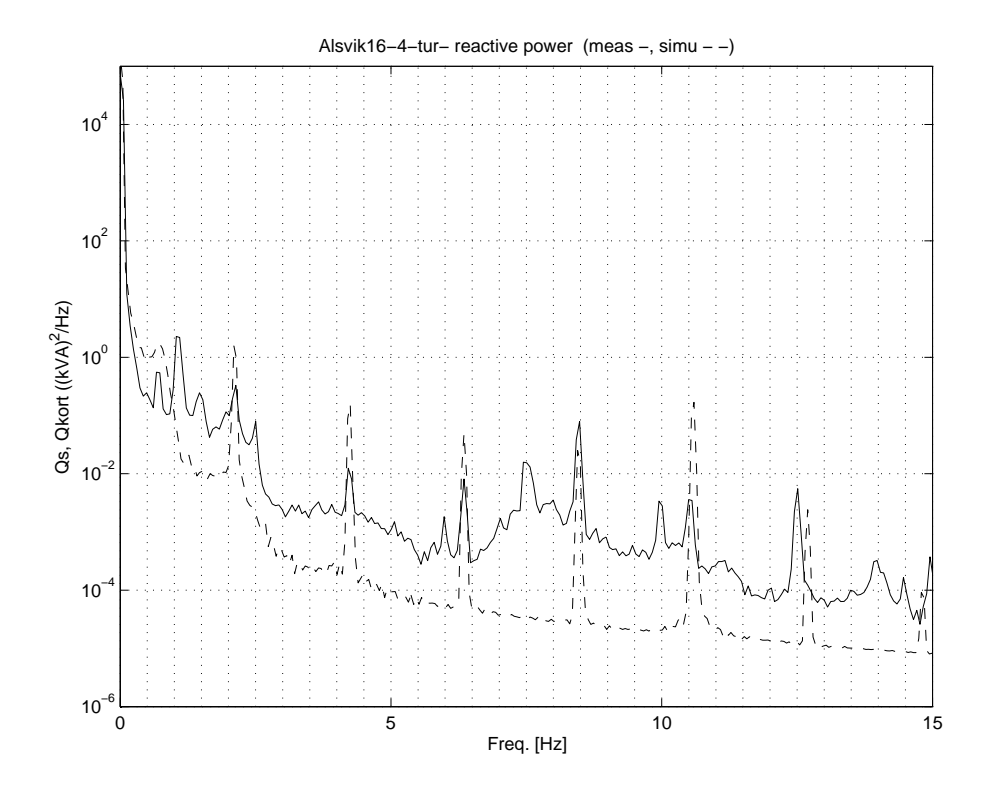


Figure 18: APSD of Measured (WD285WS100-1) and Simulated Reactive Power of Turbine 4

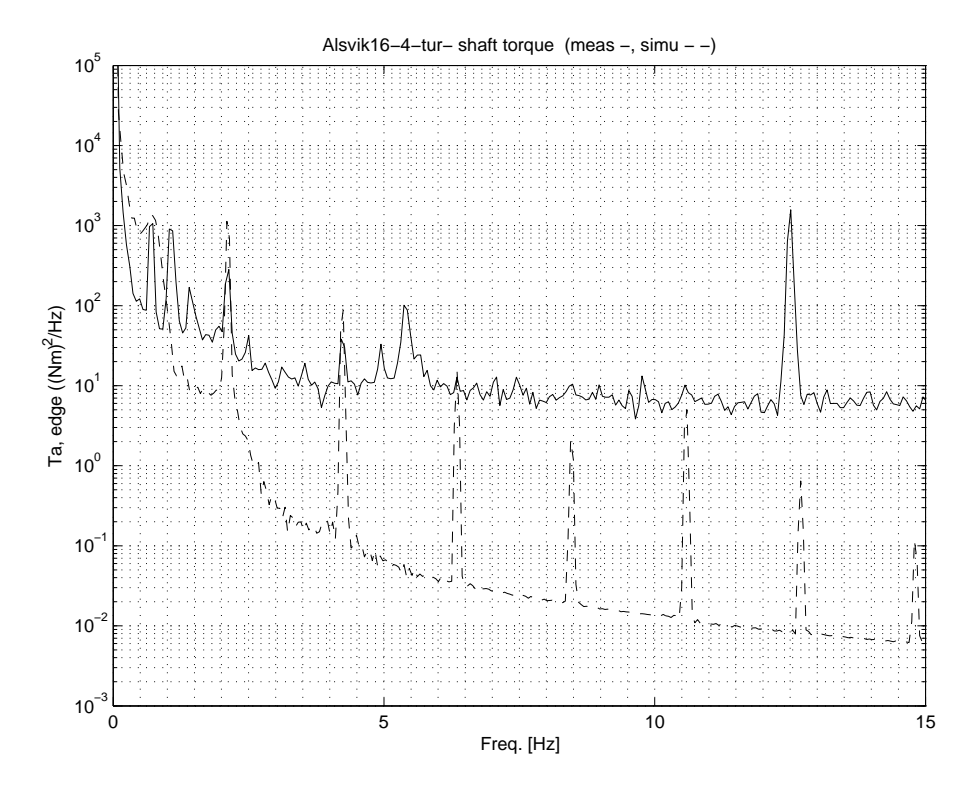


Figure 19: APSD of Measured (WD285WS100-1) and Simulated Mechanical Torque (LSS) of Turbine 4

6.3 Validation 2 - measurement set 3: Alsvik normal operation, 256 Hz sample frequency, voltage from grid model

Table 6: Measurement set 3: Alsvik normal operation, 256 Hz sample frequency

Sample frequency 256 Hz		
WS_1	Wind speed at bottom of rotor disc (m/s)	
WS_2	Wind speed at hub height (m/s)	
WS_3	Wind speed at top of rotor disc (m/s)	
WD	Wind direction) (Deg)	
u_1	Voltage phase 1	
u_2	Voltage phase 2	
u_3	Voltage phase 3	
i_{21}	Current turbine 2 phase 1	
i_{22}	Current turbine 2 phase 2	
i_{23}	Current turbine 2 phase 3	
i_{31}	Current turbine 3 phase 1	
i_{32}	Current turbine 3 phase 2	
i_{33}	Current turbine 3 phase 3	
i_{41}	Current turbine 4 phase 1	
i_{42}	Current turbine 4 phase 2	
i_{43}	Current turbine 4 phase 3	

Table 6 lists the measured variables and the sample frequencies of measurement set 3. This set includes voltage and current measurements at a sufficiently high sample rate to determine APSDs. Mechanical measurements are not included in this set. The wind speed and wind direction have been measured and the turbulence level was calculated from the measurement. The $I_{15class}$ level of 6% (std = 0.55 m/s) is low but not unrealistically low.

The individual phase current and voltage values $i1, ..., u_3$ will not be compared, due to the dominant 50 Hz component, instead the effective phase-phase voltage and the effective current will be used:

$$u_{eff, ph-ph} = \sqrt{u_1^2 + u_2^2 + u_3^2} = \sqrt{3}u_{eff, ph-0}$$

$$i_{eff, ph-ph} = \sqrt{i_1^2 + i_2^2 + i_3^2} = \sqrt{3}i_{eff, ph-0}$$
(2)

$$i_{eff, ph-ph} = \sqrt{i_1^2 + i_2^2 + i_3^2} = \sqrt{3}i_{eff, ph-0}$$
 (3)

(4)

assuming symmetrical conditions and absence of harmonic distortion. As in the previous section, APSD values will be compared, since the instantaneous value will differ due the problem of assessing the instantaneous rotor effective wind speed (see section 5.1). A second option is to compare the APSDs of the dq-reference frame voltages u_d and u_q calculated from the measurements and the simulation. The effect of comparing dq-reference frame values instead of equivalent values is expected to be negligible.

Table 7: Validation 2 - measurement set 3 : Alsvik normal operation, measurement and model specification (Tx = turbine number x)

Alsvik measurements validation 2		
Set 3	D6-F372.I32	
	direction = 281 deg, av. wind speed = 10 m/s	
Length	1200 s	
Variables and sample rate	phase to zero voltages: 256 Hz	
	phase currents T2, T3 and T4: 256 Hz	
Model specification		
Wind input	10 m/s constant + rotor effective wind	
Turbulence level	I15class = 0.06	
Wake correction	no	
Parameters deviation from Chalmers specs	none	
Grid connection	13.8 kV SM, 13.8 kV, 150 kV and 10 kV grid, 415 V turbine	
Simulink model version	CSS-3-turb-Alsvik-12.mdl	
Nr. of turbines in model	3	

Table 7 lists the model specifications for the second validation exercise. Figure 20 shows the APSDs of the measured and simulated effective current of turbine 2 (turbine 1 is not in operation in this measurement). The APSD levels of the current from 0-4 Hz correspond better than the levels of the power, reactive power and torque in validation 1. Some peaks in the measurement (1, 7.5 and 16.8 Hz) are still missing in the simulation and the frequency content above 4 Hz is still too low.

Figures 21 and 22 give the spectra of the currents of turbine 3 and 4, which roughly show the same deviations as for turbine 2. The differences between the APSDs of the currents of the different turbines may be caused by different wind conditions or the distance to the Point of Common Coupling (PCC). In the model, these differences also exist, the exact layout and properties of the cable connection to the PCC is not known however.

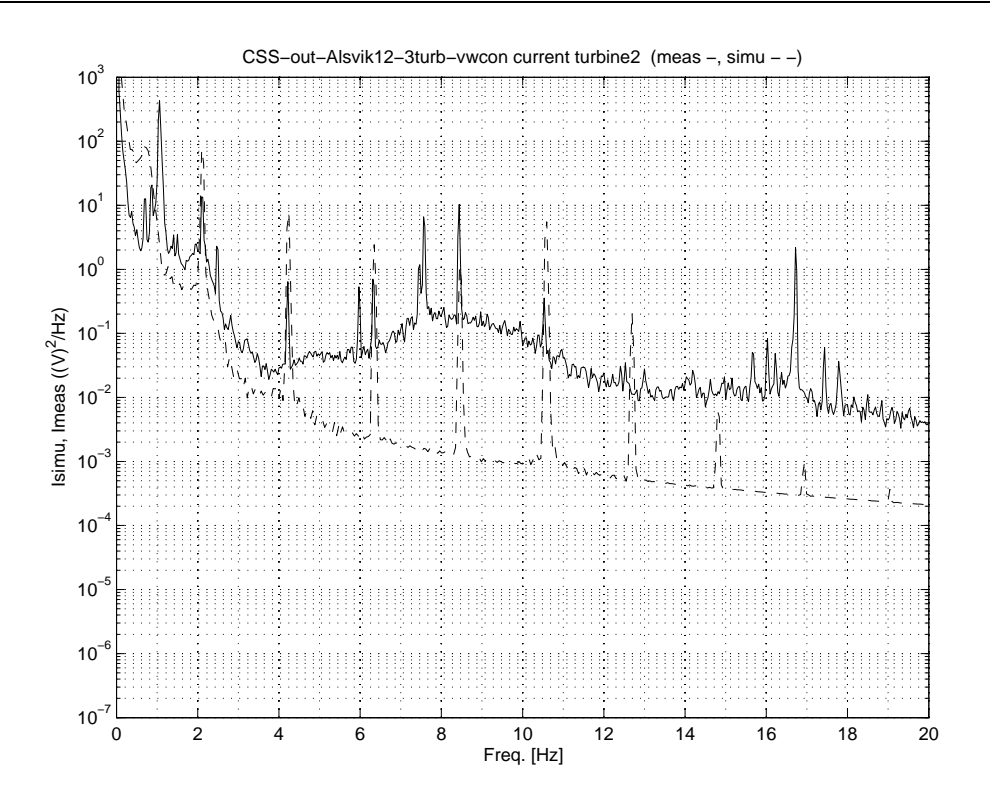


Figure 20: APSD of the measured and simulated effective current of turbine 2 (voltage from grid model)

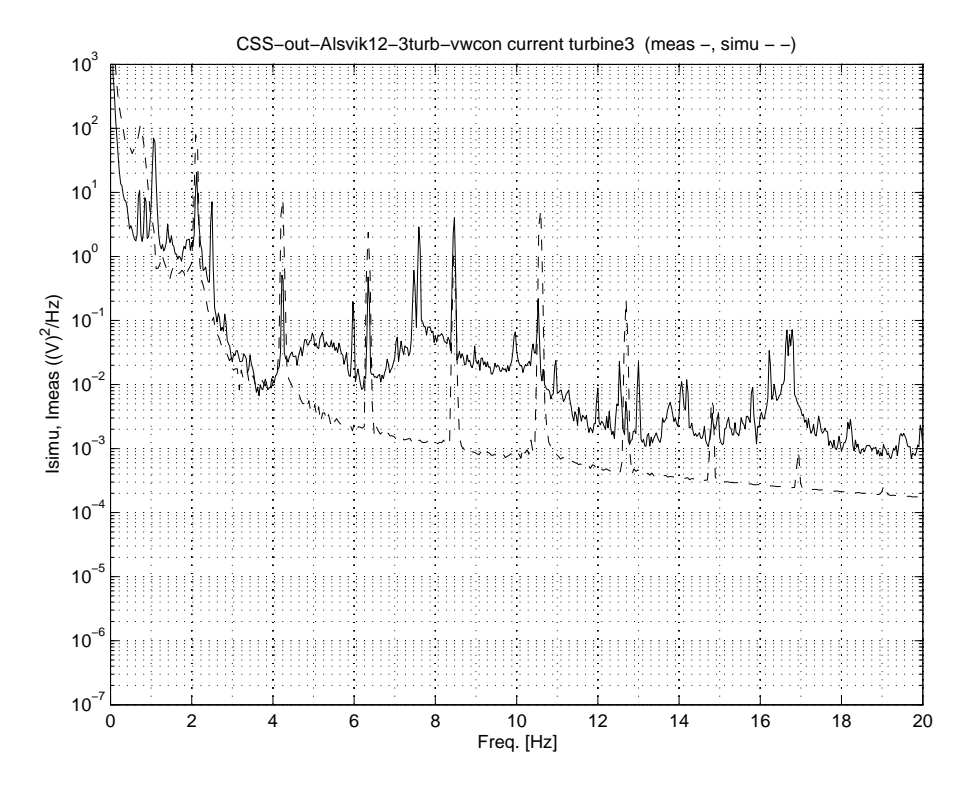


Figure 21: APSD of the measured and simulated effective current of turbine 3 (voltage from grid model)

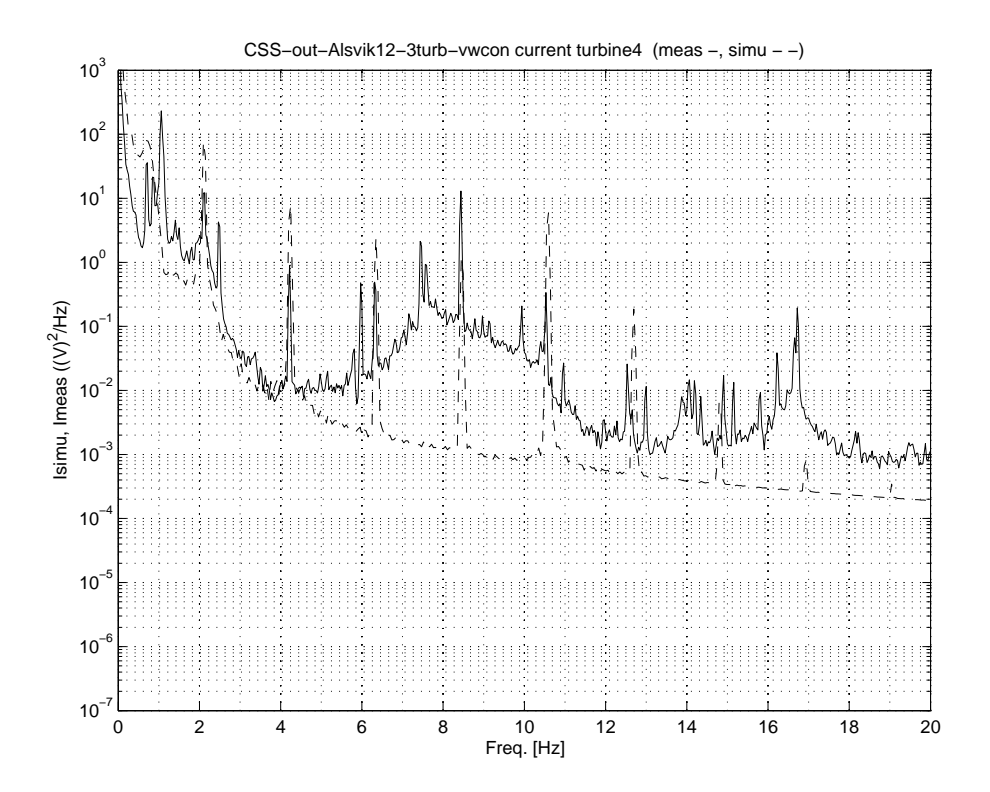


Figure 22: APSD of the measured and simulated effective current of turbine 4 (voltage from grid model)

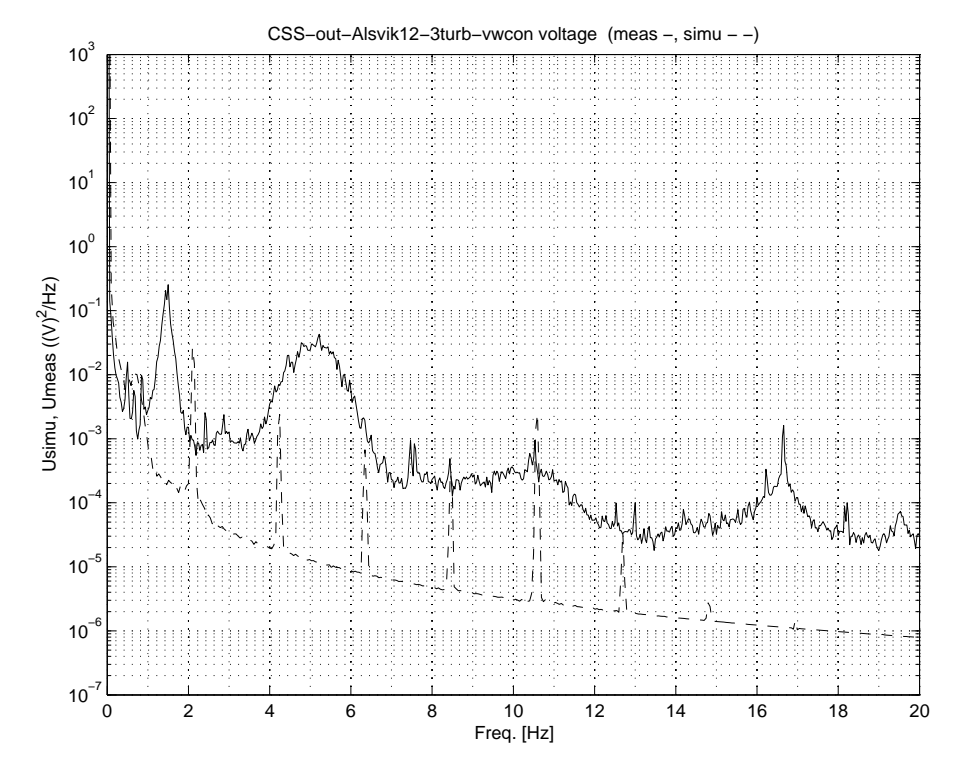


Figure 23: APSD of the measured and simulated effective voltage

Figure 23 gives the frequency content of the measured and the simulated voltage. It is clear that the level of oscillations in the measured voltage above 1 Hz is significantly higher, about a

factor 10-100 (squared). A plausible reason for the difference is the inherent level of oscillation of the grid voltage, primarily caused by the changes in electrical loads on the grid and the effect of the grid voltage and frequency controllers trying to keep the voltage and frequency at the required level. There are a number of peaks in the measured voltage APSD, 1.5, 5 and 16.8 Hz, of which the origin is unknown. In the next validation case, the measured voltage will be used as input in the simulation.

6.4 Validation 3 - measurement set 3 : Alsvik normal operation, 256 Hz sample frequency, measured voltage input

A measured voltage at the turbine terminals is not an independent variable, since there can be a strong correlation with the rotor effective wind speed, especially for a constant speed turbine. In the validation of a dynamic model, input variables which are correlated should be handled with care, especially if one of these input variables is not known. The concequences of using the measured voltage as an input in validating the model of the Alsvik wind farm are investigated in appendix A. It is concluded that the error caused by using the measured voltage as input is small, due to the low correlation between the voltage and rotor effective wind speed. This is the result of two circumstances:

- during the Alsvik measurements multiple turbines are in operation;
- a substantial amount of noise on the voltage signal can be attributed to load changes in the grid.

In the validation presented in this section, the measured voltage is used as an input for the Alsvik wind farm model. Simulation conditions can be found in table 8.

Table 8: *Validation 3 - measurement set 3 : Alsvik normal operation, measurement and model specification (measured voltage as input)*

Alsvik measurements validation 3	
Set 3	D6-F372.I32
	direction = 281 deg, av. wind speed = 10 m/s
Length	1200 s
Variables and sample rate	phase to zero voltages: 256 Hz
	phase currents T2, T3 and T4: 256 Hz
Model specifi cation	
Wind input	10 m/s constant + rotor effective wind
Turbulence level	I15class = 0.06
Wake correction	no
Parameters deviation from Chalmers specs	none
Grid connection	measured voltage is input
Simulink model version	CSS-3-turb-Alsvik-14-no-grid.mdl
Nr. of turbines in model	3

Figure 24, 25 and 26 give the APSDs of the current of turbine 2, 3 and 4. The correspondance is much better than in section 6.3 with the voltage calculated by a grid model. Turbine 3 gives the best match, therefore it is expected that the voltage was measured at or near turbine 3. Level and shape of the measured and simulated APSD of the turbine 3 current are very similar, except for the range between 6-10 Hz, where the measurement is more volatile than the simulation.

This indicates that there is still something missing in the model. It can be concluded however, that using the measured voltage as an input significantly improves the simulation results.

Figures 27 to 32 give the APSDs of the power and the reactive power calculated from the measurements and the simulation. Again the match is best for turbine 3. The APSDs of the power of turbine 3 only differ in the 6-10 Hz range, for the reactive power the agreement for turbine 3 is very good over the complete frequency range (figure 31).

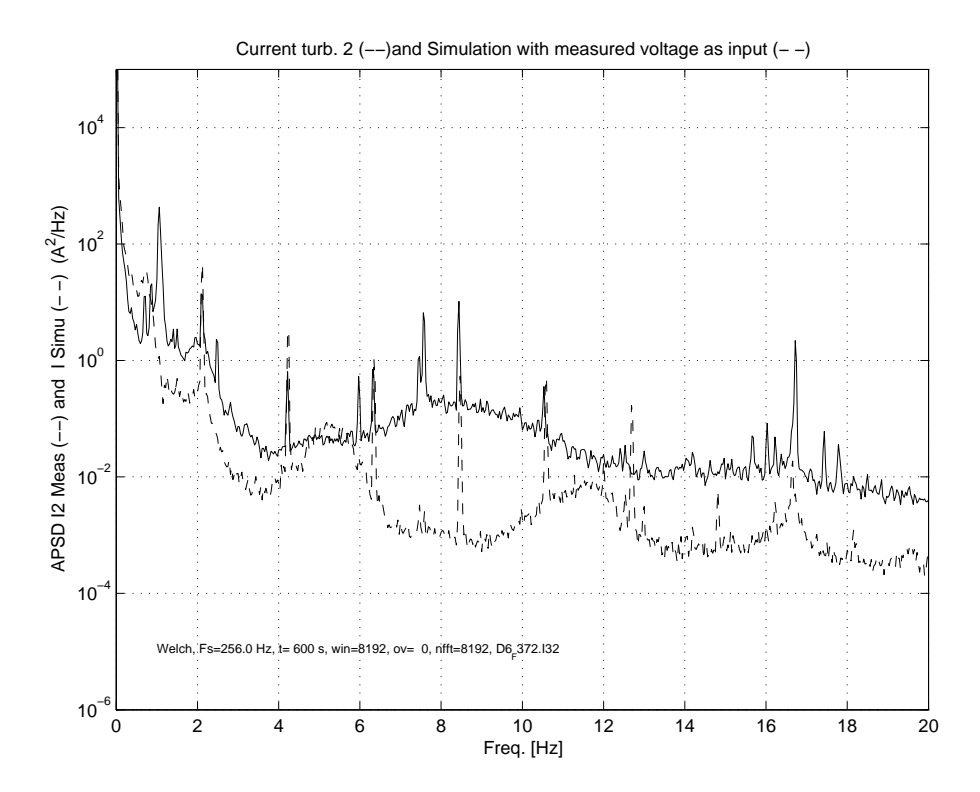


Figure 24: APSD of the measured effective current of Alsvik turbine 2 and simulated current (measured voltage as input)

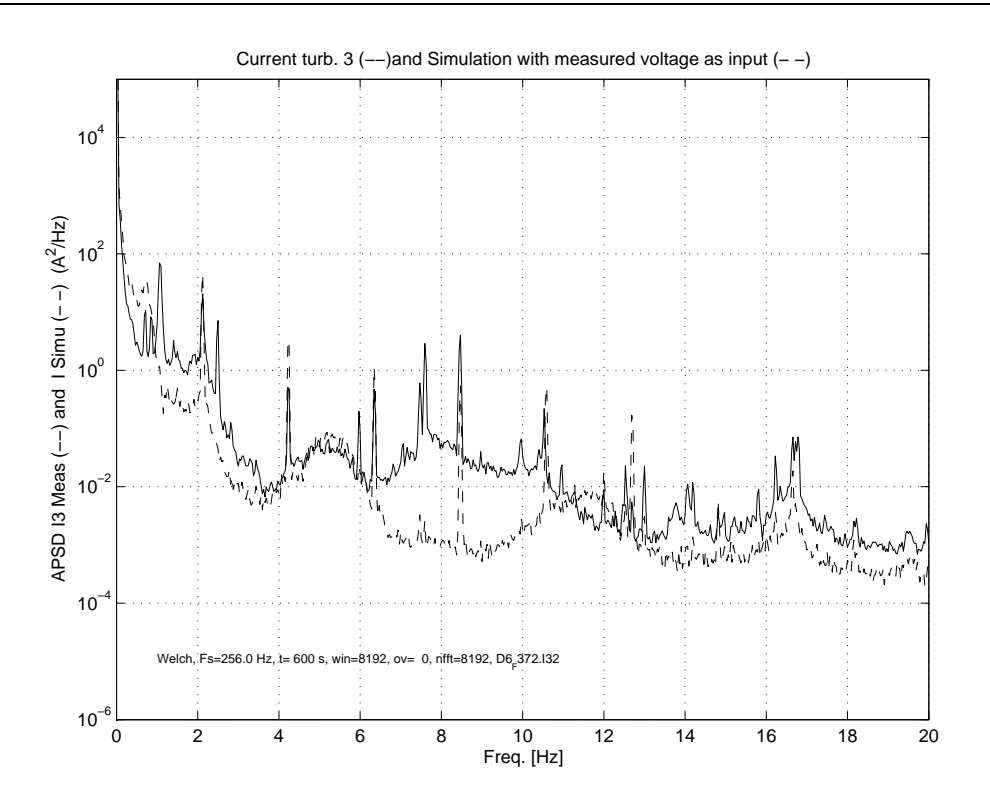


Figure 25: APSD of the measured effective current of Alsvik turbine 3 and simulated current (measured voltage as input)

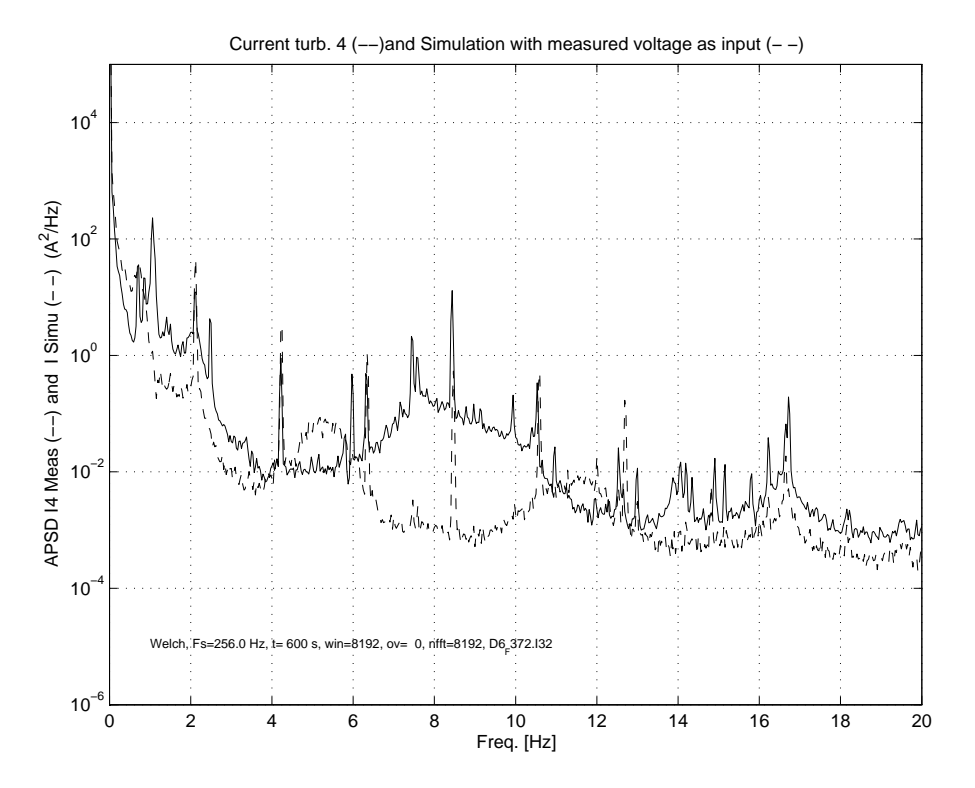


Figure 26: APSD of the measured effective current of Alsvik turbine 4 and simulated current (measured voltage as input)

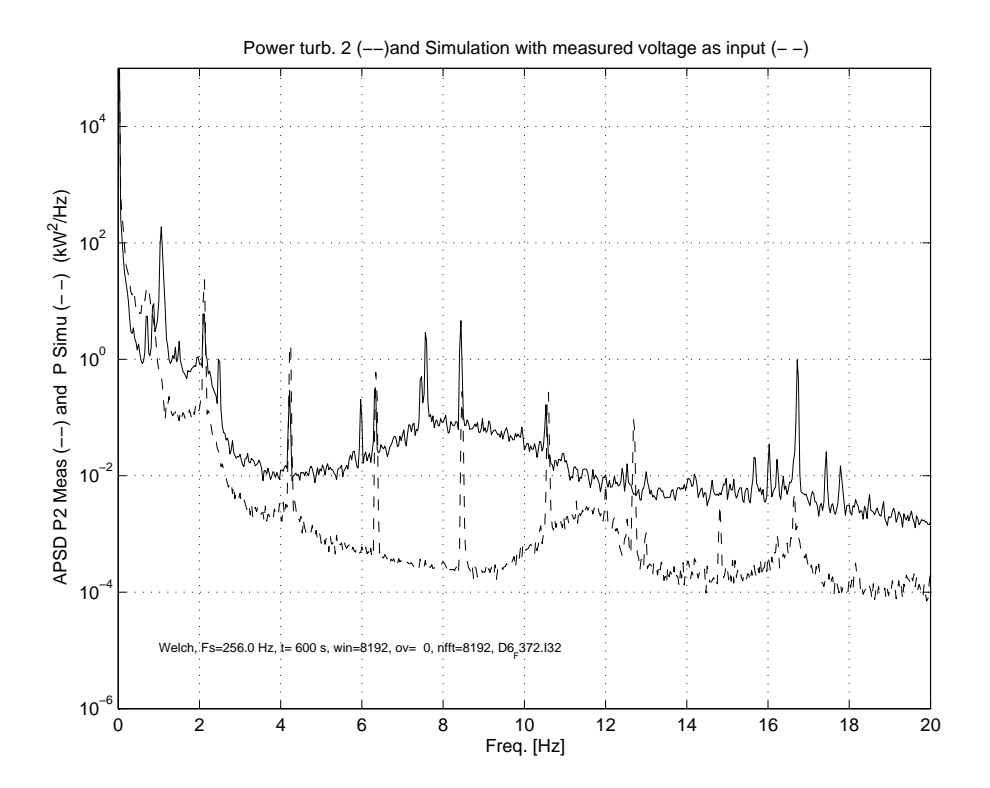


Figure 27: APSD of the measured power of Alsvik turbine 2 and simulated power (measured voltage as input)

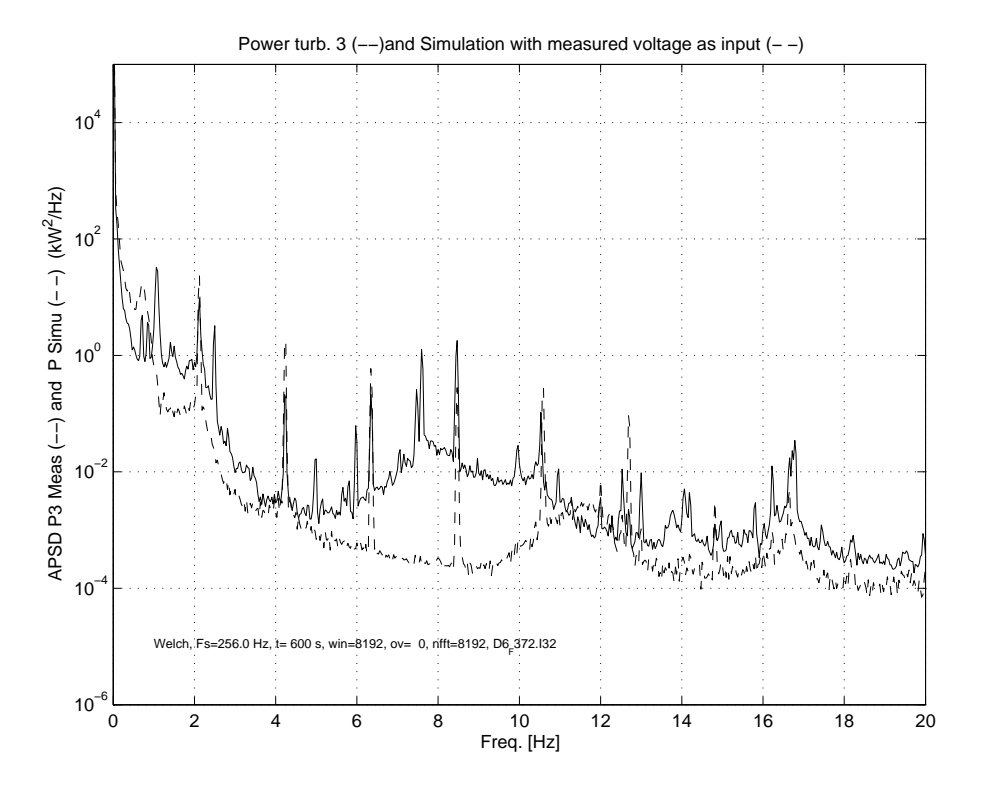


Figure 28: APSD of the measured power of Alsvik turbine 3 and simulated power (measured voltage as input)

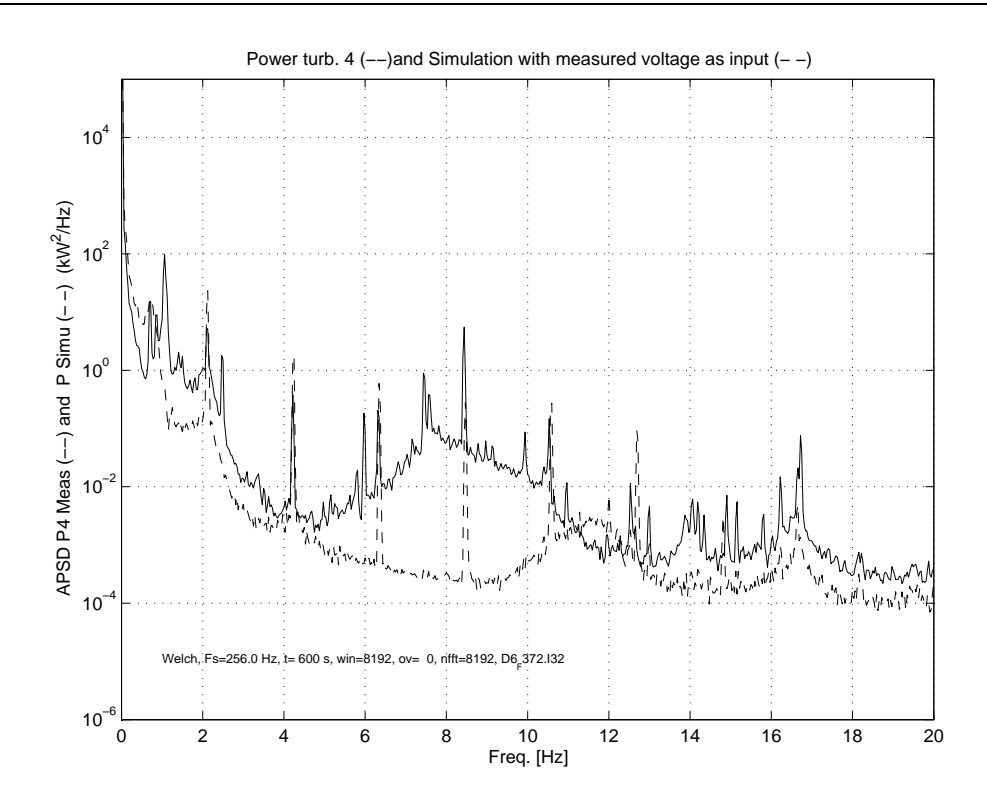


Figure 29: APSD of the measured power of Alsvik turbine 4 and simulated power (measured voltage as input)

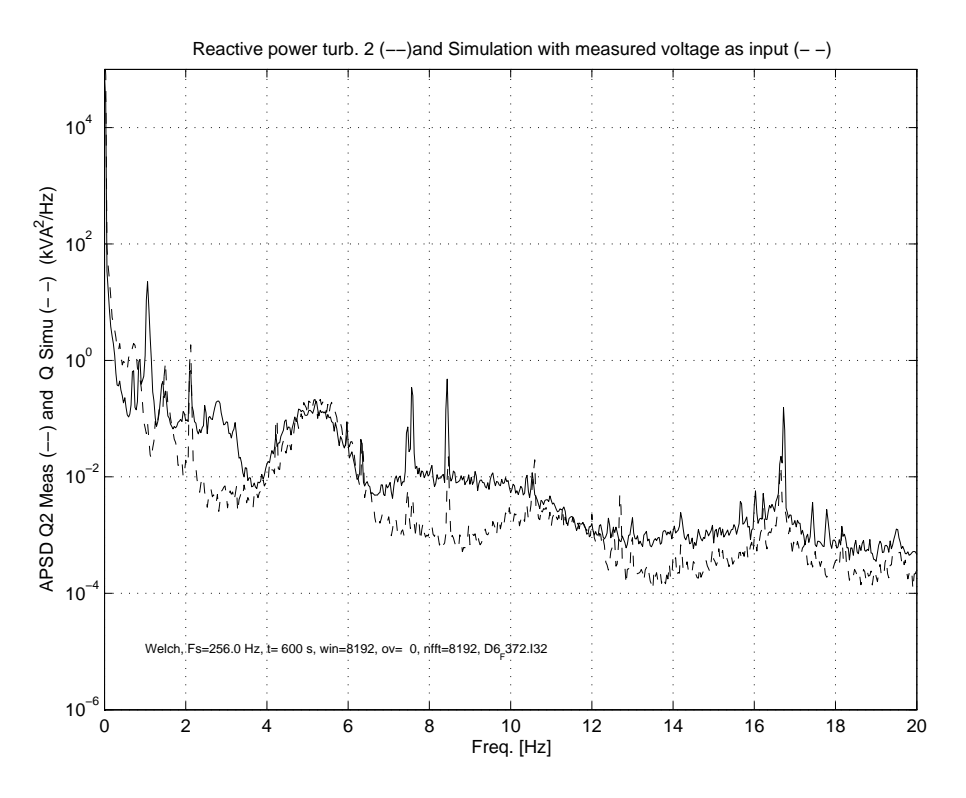


Figure 30: APSD of the measured reactive power of Alsvik turbine 2 and simulated reactive power (measured voltage as input)

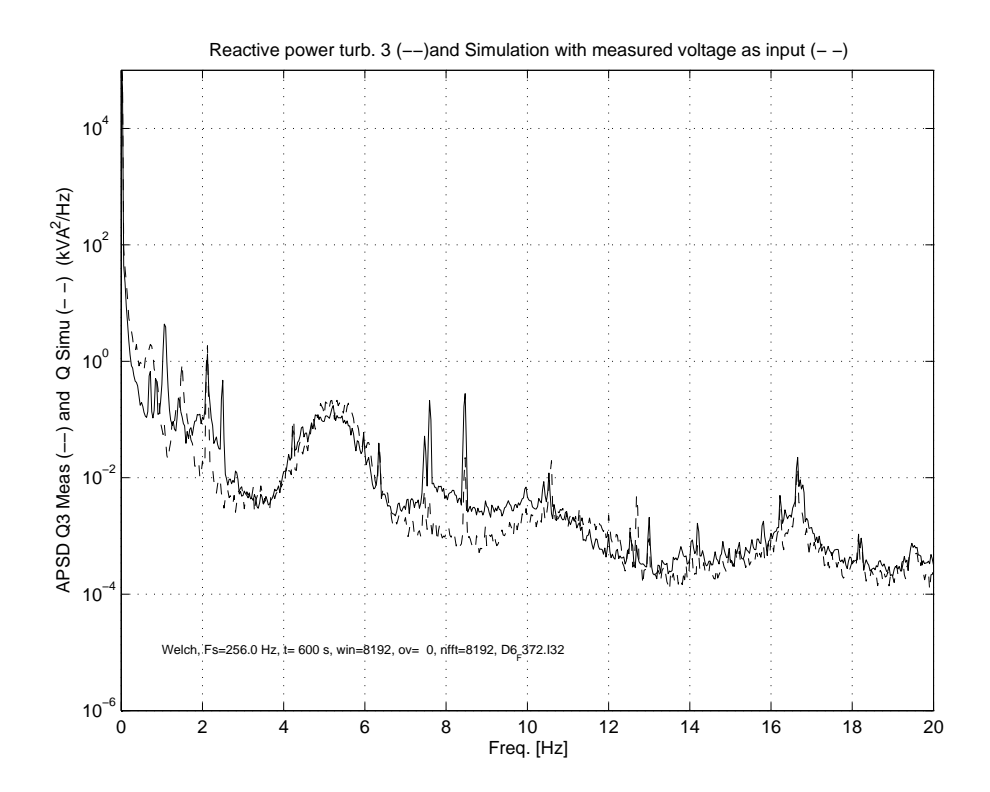


Figure 31: APSD of the measured reactive power of Alsvik turbine 3 and simulated reactive power (measured voltage as input)

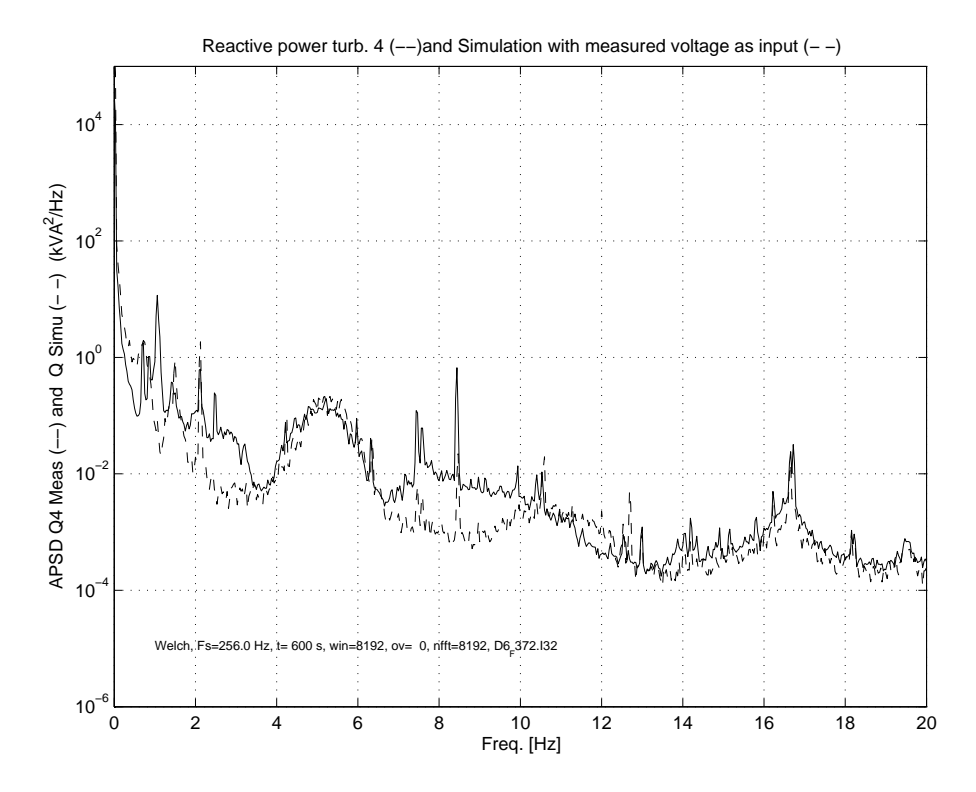


Figure 32: APSD of the measured reactive power of Alsvik turbine 4 and simulated reactive power (measured voltage as input)

6.5 Validation 4 - measurement 4: Alsvik Turbine 3 voltage dip

Table 9: Validation 4 - measurement set 4: Alsvik Turbine 3 voltage dip, measurement and model specification:

Alsvik measurements validation 4			
Set 4	DIPDATA.asc		
Length	4 s		
Variables and sample rate	phase voltages and phase currents turbine 3: 256 Hz		
Model specification			
Wind input	4.5 m/s constant + rotor effective wind		
Turbulence level	I15class = 0.06		
Wake correction	no		
Parameters deviation from Chalmers specs	none		
Grid connection	measured voltage dip is input		
Simulink model version	CSS-turb-Alsvik-13-no-grid.mdl		

Table 9 list the conditions for the simulation of the voltage dip at turbine 3 of the Alsvik wind farm. Only turbine 3 is in operation during the dip. The instantaneous phase to zero voltages of all three phases were measured with a sample frequency of 256 Hz. These voltage values are either converted to an instantaneous effective voltage which is used as u_q or the instantaneous phase voltages are transformed to a synchronously rotating reference frame, resulting in variable u_d and u_q values. In the latter case, the grid frequency is assumed to be 50 Hz. For a short measurement this is expected to be no problem. Since the sample frequency is only 256 Hz, the values are interpolated in the simulation.

Case 1: assuming
$$u_q = u_{eff, ph-ph}, u_d = 0$$

In the first case, it is assumed that the q-voltage equals the effective phase to phase voltage $u_{eff, ph-ph}$ calculated from the measured instantaneous phase to zero voltages u_1, u_2, u_3 :

$$u_q = u_{eff, ph-ph} = \sqrt{u_1^2 + u_2^2 + u_3^2} = \sqrt{3}u_{eff, ph-0}$$
 (5)
 $u_d = 0$ (6)

$$u_d = 0 (6)$$

The assumption is equivalent to an initial angle between voltage phasor and reference frame of zero and the assumption that this angle does not change, i.e. stator voltage phasor is not moving with respect to the dq-reference frame. These assumptions are not necessarily true but since the position of the voltage phasor can not be derived from the measurement without making an assumption, the most simple choise was made for case 1.

Since $u_{eff, ph-ph}$ contains a 50 Hz ripple, caused by a slight difference in the amplification of the voltage in phase 1, 2 and 3, a low-pass filter was applied with a cut-off frequency of 40 Hz. The filter leads to a small disturbance in the initial part of the transient: a small initial peak and the actual dip is less deep (see figure 33).

Figure figure 34 compares the measured and simulated effective current. The main peak in the simulated effective current is smaller than in the measurement and has opposite direction. The peaks in power and reactive power are also significantly smaller, see figure 35 and 36. The reduced level of the peaks can partly be explained by a slightly smaller voltage peak, caused by the filtering. The main oscillation frequency is about the same in measurement and in simulation. It can be concluded that the match between measurement and simulation is not that good.

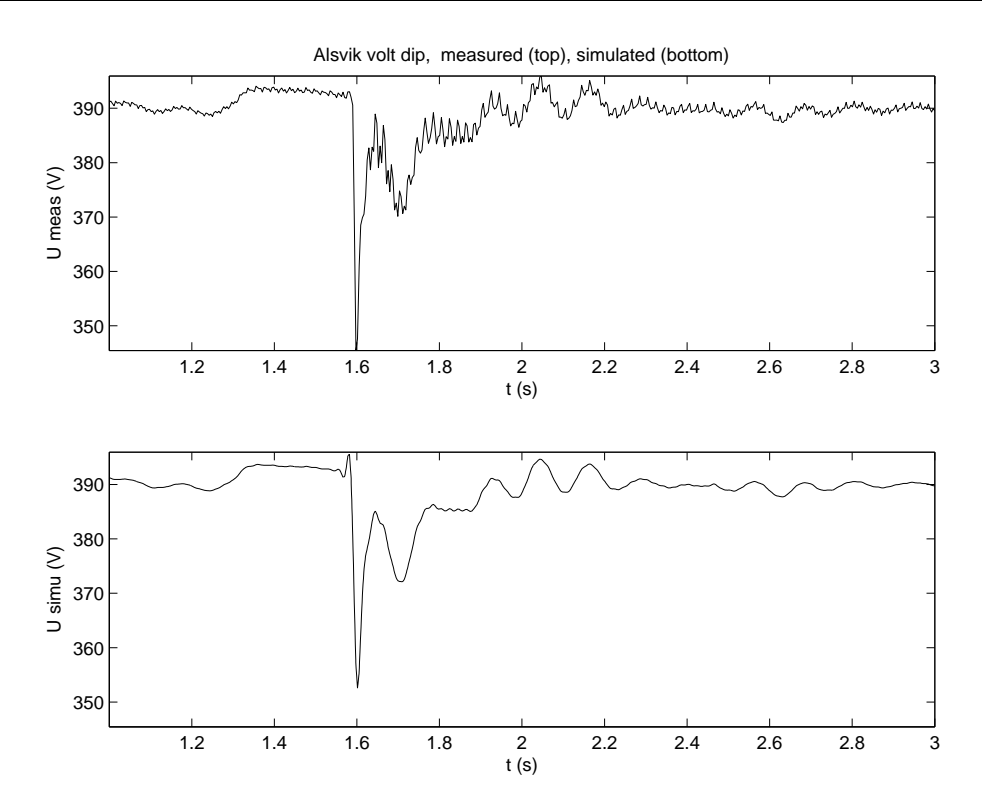


Figure 33: Alsvik voltage dip, measured (top) and filtered simulated effective voltage (bottom) for $u_q = u_{eff, ph-ph}$, $u_d = 0$

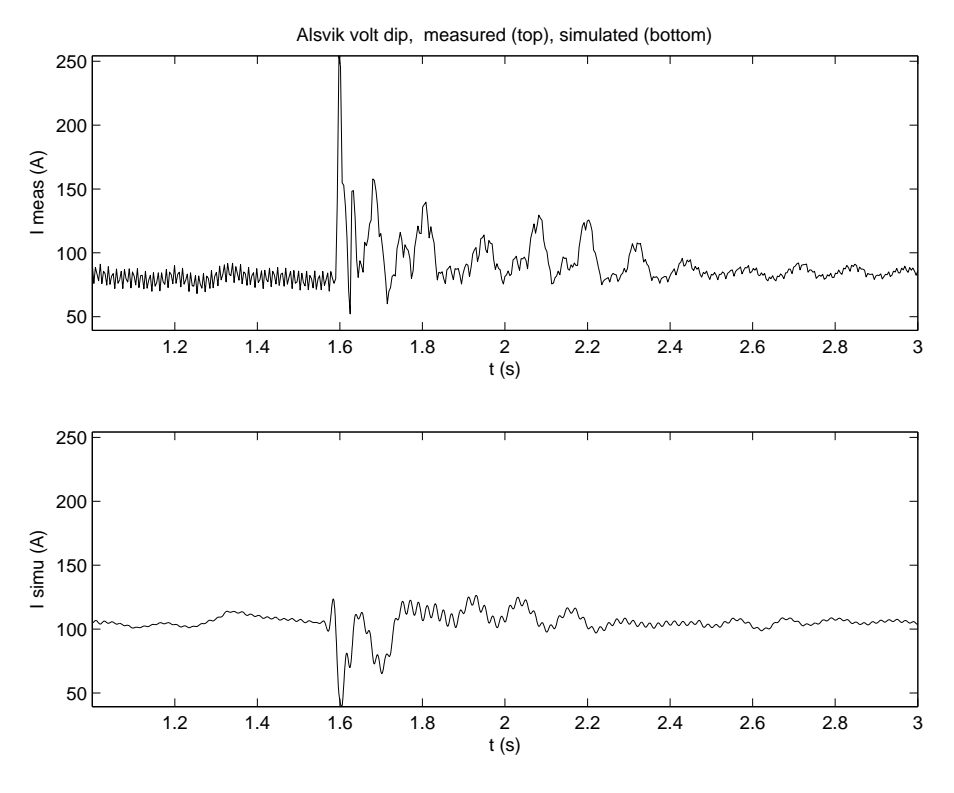


Figure 34: Alsvik voltage dip, measured and simulated effective current of turbine 3 ($u_q=u_{eff,\;ph-ph},u_d=0$)

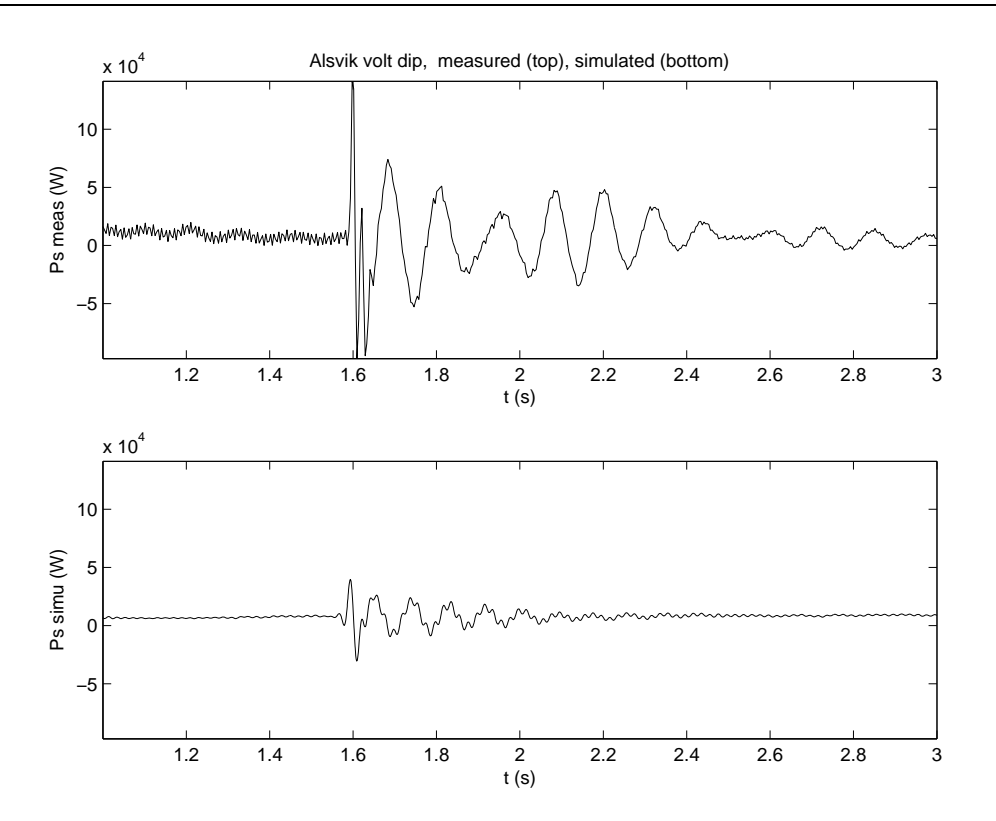


Figure 35: Alsvik voltage dip, measured and simulated power of turbine 3 ($u_q=u_{eff,\;ph-ph},u_d=0$)

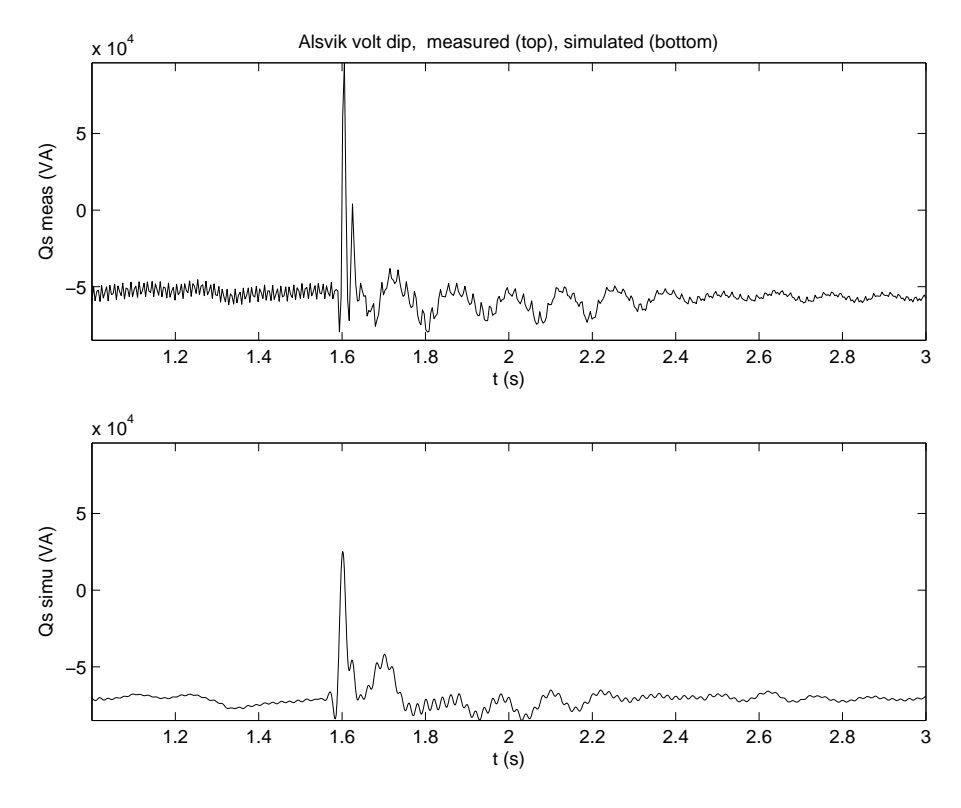


Figure 36: Alsvik voltage dip, measured and simulated reactive power of turbine 3 ($u_q=u_{eff,\;ph-ph},u_d=0$)

Case 2: assuming f = 50, u_d and u_q calculated from measurement

The assumption that the voltage phasor is not moving with respect to the reference frame may be reasonable in steady state but is probably not correct during a voltage transient. The d-and q-voltage can be calculated from the instantaneous phase to zero voltages if the frequency is known. In this way, a change in angle of the voltage phasor is taken into account. The frequency has not been measured however and is difficult to extract from the measured voltages (only a 5 samples per cycle). Therefore, the frequency is assumed to be 50 Hz and constant. Over a longer time period, this will inevitably lead to a serious error, but for the 3 seconds of the dip measurement the effect is expected to be small.

Figure 37 gives the u_d , u_q and u_0 calculated from the measured voltage. The first dip in u_q at t=0.5 s is also present in $u_{eff,\ ph-ph}$, but was not shown in figure 33. During the second dip, both u_q and u_d oscillate significantly and the angle of the voltage phasor changes, which indicates that the assumption of option 1 ($u_q = u_{eff,\ ph-ph}, u_d = 0$) is likely to produce inaccurate results.

Figure 38 compares the measured voltage and the voltage calculated from u_d and u_q only, balanced operation is assumed so the zero component is not included in the model. The effect of u_0 is small.

Figure 39 compares the measured and simulated effective current. The level of the simulated current peaks has increased, compared to option 1, and is simular to the level in the measurement. The peak in negative direction is larger however. The two main frequencies present in the measurement are also found in the simulation, only with different levels of damping. This is an indication of inaccurate modelling of the generator (fifth order model without saturation) or the mechanical transmission. Underestimation of the damping may be an important consideration when the model is used in a grid stability study.

Figures 40 and 41 compare the measured and simulated active and reactive power. The active power levels are the same, the reactive power is a bit lower in the simulation. With regard to the oscillations, the deviations observed in the current are also found in the active and reactive power. The match between simulation and measurement is much better than for the assumtion of a constant voltage phasor angle. The main deviation is the damping.

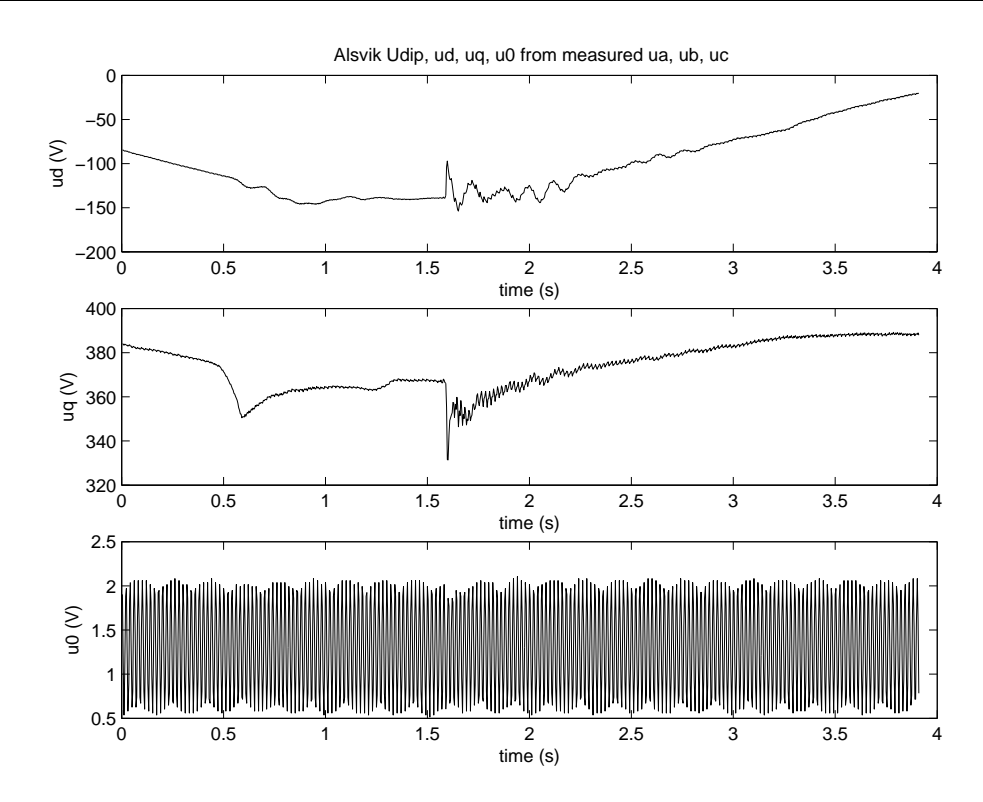


Figure 37: Alsvik voltage dip, u_{dq0} calculated from measured phase voltages (f=50~Hz constant)

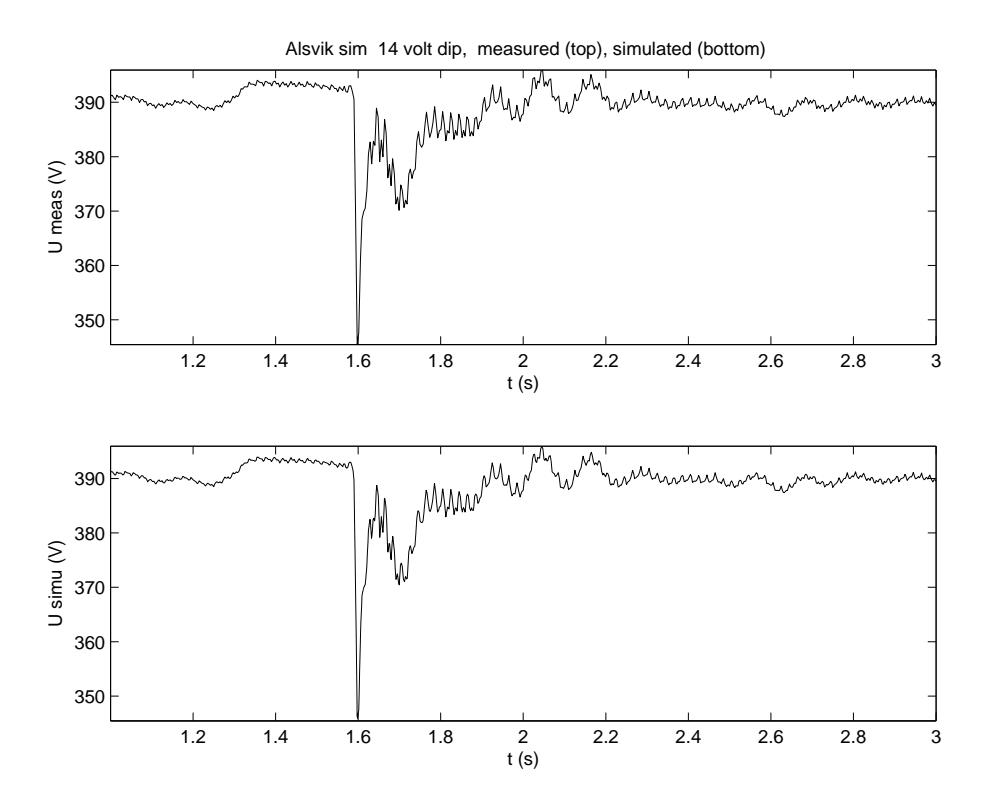


Figure 38: Alsvik voltage dip, measured and simulated effective voltage (f = 50 Hz constant)

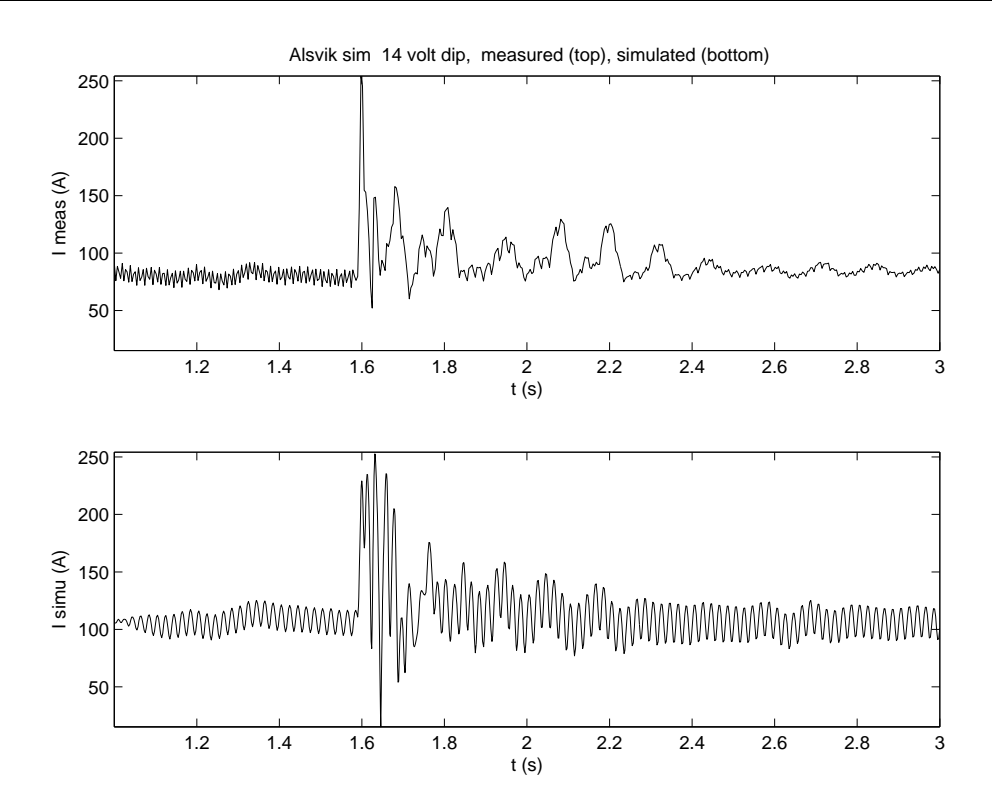


Figure 39: Alsvik voltage dip, measured and simulated effective current of turbine 3 (f = 50 Hz constant)

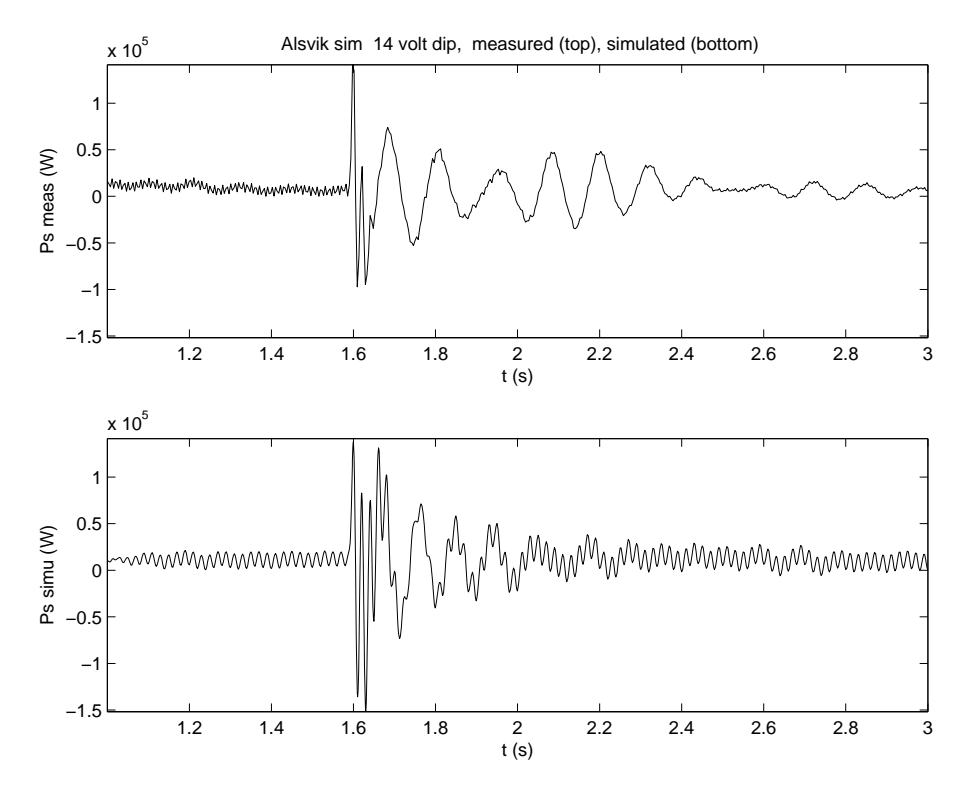


Figure 40: Alsvik voltage dip, measured and simulated power of turbine 3 (f = 50 Hz constant)

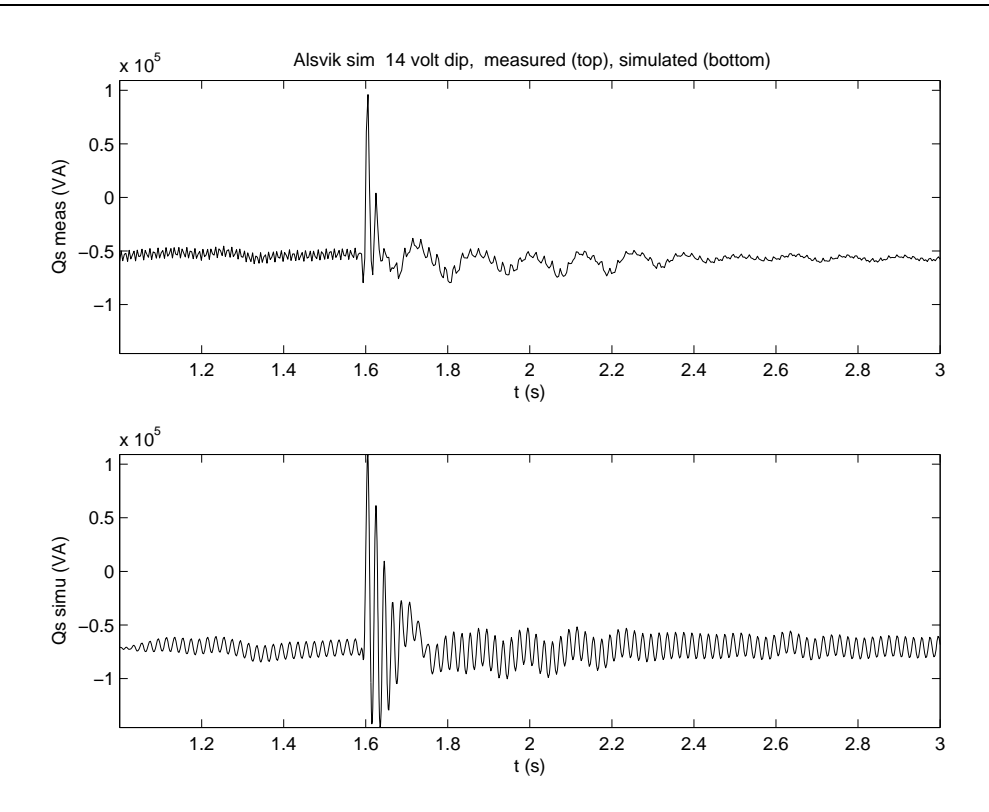


Figure 41: Alsvik voltage dip, measured and simulated reactive power of turbine 3 (f = 50~Hz constant)

7 CONCLUSIONS

For the validation of the dynamic model of the Alsvik constant speed stall wind farm, measurements and simulation results have been compared. The validation process was hindered by a number of problems:

- the time series of the rotor effective wind speed during the measurement is not known, which makes comparing time series of measured and simulated variables impractical;
- voltage and wind speed measurements are not independent and this will result in errors when the voltage is used as an input to determine the frequency response by simulation.

For the first problem a work around is found by comparing the frequency response of measurements and simulations. Frequency domain representations are an excellent way to obtain the properties of dynamic models. The second problem requires the quantification of the coherence of voltage and wind speed. It was shown that the measured voltage is acceptable as an input for the Alsvik validation case.

Three measurement sets have been used for the validation of the Alsvik constant speed stall wind farm model. In the first set, mainly mechanical parameters have been recorded. The voltage was not measured and a grid model was used to generate the voltage at the point of common coupling of the wind farm. The simulation results with for measurement set are not that good. There are significant differences between the measured and the calculated APSDs of the electric power, reactive power and mechanical torque. Some oscillations are missing and the level of oscillation above 1 Hz is underestimated. These discrepancies can be caused by several factors:

- inaccurate mechanical parameters, for instance the stiffness and damping of the tower are not well known;
- incomplete modeling of the turbine rotor: only a simple steady state representation of the rotor is used, blade lead-lag and flap oscillations are absent in the simulation;
- an insufficient level of detail of the models of the electrical components of the wind farm (no saturation, simplified transformer and cable representations);
- an inadequate representation of the grid (a single synchonous generator, no grid load changes).

Especially the effect of the simplified rotor model and the grid model may be important. The autonomous variation of the grid voltage is not present in the grid model. The voltage in the simulation is much less variable than in the measurement. Including electric load changes in the grid or using the measured voltage as an input is expected to give a better result.

The second measurement set included measurements of the instantaneous phase voltages and currents and is used to investigate the effect of the grid voltage variation on the simulation results. First, the Alsvik farm was simulated with the same grid model as in set 1 and these results are better than for set 1. Predicting the mechanical variables seems to be more difficult than predicting the electrical variables. When the measured voltage is used as input, the results are significantly better, especially for turbine 3. The only difference between measurement and simulation is a broad peak in the spectra of current and power around 8 Hz. The reactive power spectra of measurement and simulation are practically the same. It would have been useful to

46 ECN-E-07-007

use the measured voltage as input in set 1 as well, to see to what extent this improves the result for the mechanical variables, but unfortunately this voltage is not available.

The third measurement available for validation is a voltage dip. For this short measurement of about 3 seconds, the instantaneous value of the rotor effective wind speed is not that important and time series of measurement and simulation can be compared. To simulate the dip, the measured voltage is the main model input and has to be converted to the dq0-reference frame. Since the exact value of the frequency is not known, two assumptions have been examined: constant voltage phasor angle and constant voltage phasor rotational frequency. The second assumption gives the best result. The oscillation frequencies and the maximum peak value are estimated with reasonable accuracy, the damping of the oscillations is different.

The validation of the model of the Alsvik wind farm showed that:

- the frequency response results of the electrical variables are good if the measured voltage is used as input instead of using a grid model;
- the frequency response results of mechanical variables are less good, which may partly be caused by variation of the grid voltage, which could not be used as input because it was not measured:
- the results for the voltage dip were quite good, with some mismatch in the damping.

48 ECN-E-07-007

REFERENCES

- [1] I. Carlen. Some answers . email, 2 june 2004.
- [2] E. Djerf and H. Mattsson. Evaluation of the software program Windfarm and comparison with the measured data of Alsvik. Technical Report FFA TN 2000-30, FFA, 2000.
- [3] Matlab. Signal Processing Toolbox User's Guide. MathWorks Inc., Natick, MA, 2000.
- [4] D.E. Newland. Random vibrations and spectral analysis. Longman, London, 1975.
- [5] J.T.G. Pierik, M.E.C. Damen, P. Bauer, and S.W.H. Electrical and control aspects of offshore wind farms, Phase 1: Steady state electrical design and economic modeling, Vol. 1: Project results. Technical Report ECN-CX-01-083, ECN Wind Energy, 2001.
- [6] J.T.G. Pierik and J. Morren. Validation of dynamic models of wind farms (Erao-3): Executive summary, benchmark results and model improvements. Technical Report ECN-E-07-006, ECN, 2007.
- [7] J.T.G. Pierik and J. Morren. *Variable Speed Wind Turbine Dynamic Model Validation; JWT measurements and simulations.* Technical Report ECN-E-07-008, *ECN*, 2007.
- [8] J.T.G. Pierik, J. Morren, E.J. Wiggelinkhuizen, S.H.W. de Haan, T.G. van Engelen, and J. Bozelie. *Electrical and Control Aspects of Offshore Wind Turbines II (Erao-2). Volume 1: Dynamic models of wind farms*. Technical Report ECN-C--04-050, ECN, 2004. available at the web site of ECN (*www.ecn.nl*, use search option).
- [9] J.T.G. Pierik, J. Morren, E.J. Wiggelinkhuizen, S.H.W. de Haan, T.G. van Engelen, and J. Bozelie. *Electrical and Control Aspects of Offshore Wind Turbines II (Erao-2). Volume 2: Offshore wind farm case studies*. Technical Report ECN-C--04-051, ECN, 2004. available at the web site of ECN (*www.ecn.nl*, use search option).
- [10] J.G. Schepers. Aerodynamic modelling of Danwin 180 kW turbine. 2004.
- [11] John O. Tande, Eduard Muljadi, Ola Carlson, Jan Pierik, Ana Estanqueiro, Poul Sørensen, Mark O-Malley, Alan Mullane, Olimpo Anaya-Lara, and Bettina Lemstrom. *Dynamic models of wind farms for power system studies: status by IEA Wind R&D Annex 21*. In *Proceedings of the EWEC 2004*, London, 2004.
- [12] T. Thiringer. Data 180 kW Danwind fixed speed stall-regulated wind turbine. Information with measurement data on IEA Annex XXI e-room, 2004.
- [13] T. Thiringer. Re: Questions about the Alsvik data . email, 22 april 2004.
- [14] T.G. van Engelen, E.L. van der Hooft, and P. Schaak. Ontwerpgereedschappen voor de regeling van windturbines. Technical Report –, ECN, 2004. to be published.
- [15] T.G van Engelen and E.J. Wiggelinkhuizen. ECN design tool for control development; revised points of departure; status report. Technical report, ECN, 2002.

ECN-E-07-007 49

A VALIDATION OF MODELS USING A CLOSED LOOP MEA-SUREMENT AS INPUT

Introduction

Model validation intends to determine whether a model correctly represents the (quasi-steady) state and the dynamic behavior of a system as well as transient operation (for instance the response of the system to a fault, especially relevant for systems including electrical components). Steady state behavior and the response to a fault can be verified by comparing time series of simulations to measurements. The emphasis is on the average values of the different variables and behavior of the controllers in quasi steady state versus the extreme values and oscillations during a fault. Dynamic behavior is typically verified by comparing measurements and simulations in the frequency domain. Since a main objective of dynamic models is the development of controllers, the behavior of the model in the frequency domain should be similar to the proces behavior. If measurements are available with a high sample rate, i.e. 100 Hz or more and are of sufficient length, Auto Power Spectral Density functions (APSDs) and transfer functions can be calculated. The APSDs visualise the frequency content of individual signals, while the tranfer functions determine the dynamic relation between signals.

Model validation is limited by the available measurements and how the measurement have been taken. An important limitation can result from measurements of signals in a feedback loop, either a proces feedback loop or a control loop. This section gives a description of this problem and the concequences for the validation proces. The description focusses on a specific example, viz. validation of dynamic models of wind turbines using wind speed and voltage measurements as inputs.

Problem definition

Dynamic models of wind turbines are validated by comparing measurements of turbine variables (for instance current and power) to model results. In a wind turbine model some of the variables are treated as inputs while others are treated as output variables. The choice is not always self-evident. Typically, wind speed and voltage are model inputs and current and electric power are outputs. Wind speed can be considered as an independent variable, at least as far as the undisturbed upwind speed is concerned. The measured voltage is often the voltage at the terminals of the turbine generator and this voltage can not be considered as an independent variable, since it depends on the wind speed. A feedback relation exists between the terminal voltage and the phase current. This feedback is determined by the grid impedance.

In model validation, the measured terminal voltage is often used as an input of the model. It that case, the grid impedance and the dynamic behaviour of the grid are not included in the model. This choice will be called *open loop* model validation. The reason to take the measured voltage as input is that the grid impedance is not known and the grid voltage behind the grid impedance is not measured. In this section will be demonstrated that the direct use of the measured terminal voltage as an input will produce an error in the model outputs. This is caused by the correlation between the wind speed and the measured voltage and the fact that the (rotor effective) wind speed during the measurement is not known. The correlation also makes it impossible to determine the open loop transfer function between terminal voltage and turbine current or power. Prior to using a measured voltage as an input in an open loop model validation process, the error which will be introduced by this choice should first be quantified.

Method

First, the mathematical relations between input and output variables for a few typical cases will be investigated. From these relations it can be seen that a problem can occur, depending on the

50 ECN-E-07-007

location of input noise for a given system. Secondly, simulations with the Alsvik wind farm model, will demonstrate the effect quantitively.

The problem is related to system identification. System identification theory is used to determine the transfer functions from measurements for open and closed loop systems with noise signals entering the system at different locations. The results for a closed loop situation (the measurement) will be compared to the open loop situation (the simulation). If the transfer functions for these two situations are identical, using the closed loop measurement signal as an input in the simulation will give correct results. If the transfer functions are different, using the closed loop measurement signal as an input will result in an error.

A.1 System identification theory approach

Consider the single input-two output linear system in figure 42.

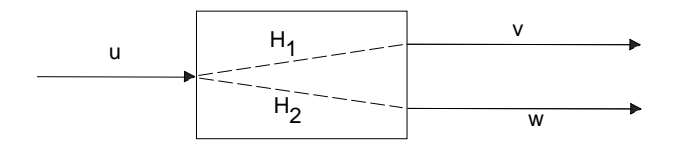


Figure 42: Schematic representation of single input-two output system

The equations governing this system are:

$$v = H_1 u
 w = H_2 u
 S_{vv} = H_1 H_1^* S_{uu}
 S_{ww} = H_2 H_2^* S_{uu}
 S_{vu} = H_1 S_{uu}
 S_{wu} = H_2 S_{uu}
 S_{vw} = H_1 H_2^* S_{uu}$$

 S_{vu} is the cross-power spectral density of (input) signal u and (output) signal v. S_{uu} is the auto power spectral density of signal u. All quantities are expressed in the frequency domain by their fourier transformation. The variable frequency ω is ommitted in all equations.

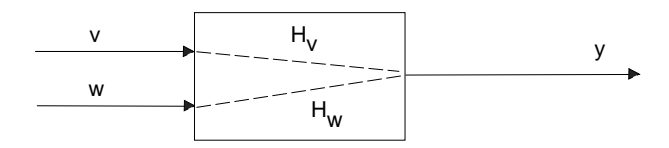


Figure 43: Schematic representation of two input-single output system

For the two-input-one-output system of figure 43 the spectral densities relate as follows. If the input signals are not independent, i.e. correlated:

$$y = H_v v + H_w w$$

$$S_{yy} = H_v H_v^* S_{vv} + H_v H_w^* S_{vw} + H_w H_v^* S_{wv} + H_w H_w^* S_{ww}$$

$$S_{yv} = H_v S_{vv} + H_w S_{wv}$$

$$S_{yw} = H_v S_{vw} + H_w S_{ww}$$

If v and w are uncorrelated (independent), S_{vw} and S_{wv} are zero so this simplifies to:

$$y = H_{v}v + H_{w}w$$

$$S_{yy} = H_{v}H_{v}^{*}S_{vv} + H_{w}H_{w}^{*}S_{ww} = |H_{v}|^{2}S_{vv} + |H_{w}|^{2}S_{ww}$$

$$S_{yv} = H_{v}S_{vv}$$

$$S_{yw} = H_{w}S_{ww}$$

The next two sections will show the effect of a feedback loop on the input-output relation of a given process, in this case a wind turbine. The effect of the location of a noise signal, viz. parallel to or in series with the feedback signal, will also be investigated.

Case 1: Verification of a turbine model using the closed loop measurement of v (voltage) with one independent input w (wind speed)

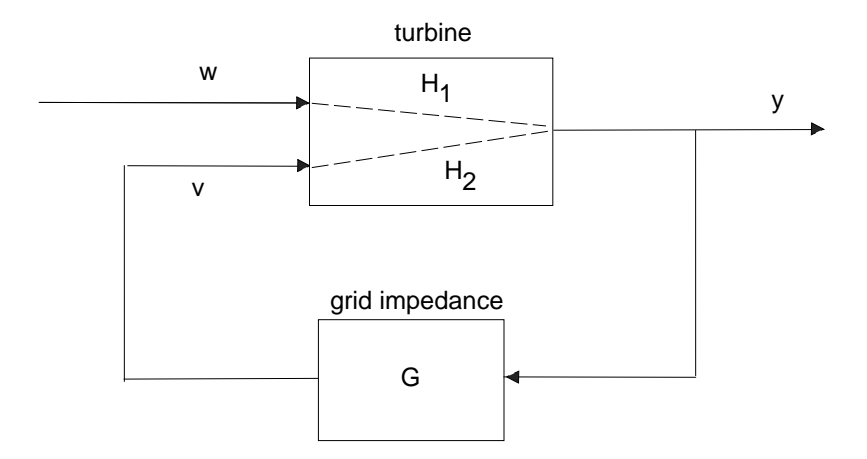


Figure 44: Schematic representation of two input-one output system with feedback

Figure 44 schematically represents a wind turbine connected to the electric grid. Turbine input signals w and v represent measured wind speed and generator terminal voltage respectively, output signal y represents the generator terminal current. The transfer function H_2 is to be validated from the measurements of v and y. H_2 is the open loop transfer function of the turbine from voltage to current.

In the validation, the measurements of v and w are used as inputs for the open loop model (so without feedback over the grid impedance) to calculate the auto power spectral desity of y. This will be compared to the APSD of the measured value of y.

The question is whether the closed loop quotient of cross power spectrum S_{yv} and the autopower spectrum S_{vv} equals the open loop quotient H_2 . If this is not the case, the (open loop)

turbine model will not give the measured (closed loop) APSD of y. Using the equations given for figure 42 and 43:

$$y = H_1w + H_2v$$

$$v = Gy = GH_1w + GH_2v$$

$$v = \frac{GH_1}{1 - GH_2}w$$

$$y = (H_1 + H_2\frac{GH_1}{1 - GH_2})w$$

Now the closed loop system of figure 44 hase been rewritten into a system with one input w and two outputs y and v, as in figure 42.

$$S_{vv} = \left(\frac{GH_1}{1 - GH_2}\right) \left(\frac{GH_1}{1 - GH_2}\right)^* S_{ww}$$

$$S_{yv} = \left(H_1 + H_2 \frac{GH_1}{1 - GH_2}\right) \left(\frac{GH_1}{1 - GH_2}\right)^* S_{ww}$$

$$\frac{S_{yv}}{S_{vv}} = \frac{\left(H_1 + H_2 \frac{GH_1}{1 - GH_2}\right) \left(\frac{GH_1}{1 - GH_2}\right)^* S_{ww}}{\left(\frac{GH_1}{1 - GH_2}\right) \left(\frac{GH_1}{1 - GH_2}\right)^* S_{ww}}$$

$$= \frac{1 - GH_2}{G} + H_2$$

$$= \frac{1}{G}$$

This demonstrates that, when measured in a closed loop, the relation between a system input and an output is not necessarily equal to the relation when measured in open loop. The closed loop measurement contains a bias term $\frac{1-GH_2}{G}$ and therefore a problem exists when the closed loop measurement of v and y are used directly to verify the open loop dynamic model of the turbine. The result could also have been achieved as follows:

$$S_{vy} = GS_{yy}$$

$$S_{yv} = G^*S_{yy}$$

$$S_{vv} = GG^*S_{yy}$$

$$\frac{S_{yv}}{S_{vv}} = \frac{G^*S_{yy}}{GG^*S_{yy}} = \frac{1}{G}$$

Case 2: Verification of a turbine model using the closed loop measurement of v (terminal voltage) with two independent inputs (wind speed w and grid voltage u)

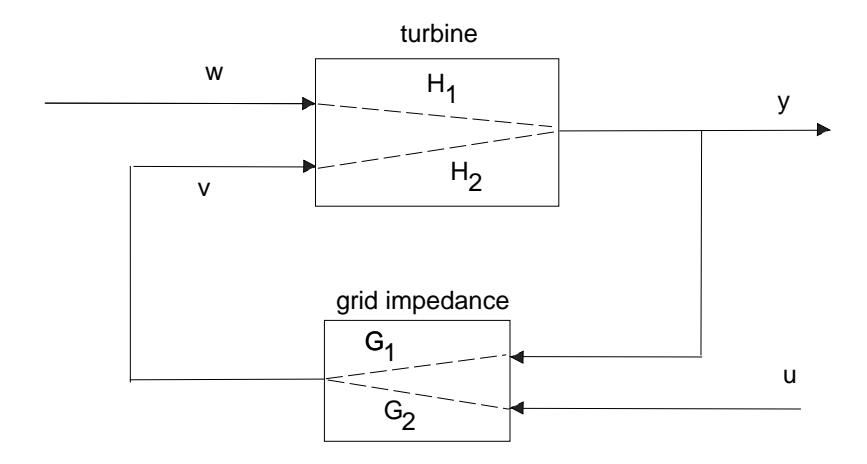


Figure 45: Schematic representation of two input-one output system with feedback and second independent input

In the second case the grid voltage behind the grid impedance u is added to the system as an additional source of noise. This noise source enters the closed loop at a different location as the first independent input (and noise source) w. The first noise source w enters the turbine model parallel to the voltage input, while the second noise source is in series with the voltage. It will be shown that this determines the effect on the model validation problem. Referring to figure 45 and rewriting to a two-input-two-output system:

$$y = H_1w + H_2v$$

$$v = G_1y + G_2u = G_1(H_1w + H_2v) + G_2u = G_1H_1w + G_1H_2v + G_2u$$

$$(1 - G_1H_2)v = G_1H_1w + G_2u$$

$$v = \frac{G_1H_1}{1 - G_1H_2}w + \frac{G_2}{1 - G_1H_2}u$$

$$y = (H_1 + \frac{G_1H_1H_2}{1 - G_1H_2})w + \frac{G_2H_2}{1 - G_1H_2}u$$

Since $S_{wu} = S_{uw} = 0$:

$$\begin{split} S_{yv} &= (H_1 + \frac{G_1 H_1 H_2}{1 - G_1 H_2}) (\frac{G_1 H_1}{1 - G_1 H_2})^* S_{ww} + (\frac{G_2 H_2}{1 - G_1 H_2}) (\frac{G_2}{1 - G_1 H_2})^* S_{uu} \\ S_{vv} &= (\frac{G_1 H_1}{1 - G_1 H_2}) (\frac{G_1 H_1}{1 - G_1 H_2})^* S_{ww} + (\frac{G_2}{1 - G_1 H_2}) (\frac{G_2}{1 - G_1 H_2})^* S_{uu} \end{split}$$

If $S_{ww} = 0$:

$$\frac{S_{yv}}{S_{vv}} = \frac{\frac{G_2H_2}{1-G_1H_2}(\frac{G_2}{1-G_1H_2})^*S_{uu}}{(\frac{G_2}{1-G_1H_2})(\frac{G_2}{1-G_1H_2})^*S_{uu}} = H_2$$

If the only independent input is the grid voltage u, which enters the closed loop at the feedback block grid impeadance, then the closed loop relation between y and v is a correct representation of the open loop proces transfer function H_2 and validation is straight forward.

If $S_{uu} = 0$:

$$\frac{S_{yv}}{S_{vv}} = \frac{(H_1 + \frac{G_1H_1H_2}{1 - G_1H_2})(\frac{G_1H_1}{1 - G_1H_2})^*S_{ww}}{(\frac{G_1H_1}{1 - G_1H_2})(\frac{G_1H_1}{1 - G_1H_2})^*S_{ww}}$$

$$= \frac{1 - G_1H_2}{G_1} + H_2$$

with the same results as before.

Conclusions from system identification theory

- 1. The architecture of the closed loop system, i.e. the signal routing, determines whether a validation problem occurs. If an input signal enters the model parallel to the feedback signal, a bias term exists. If no parallel input signal exists, there will not be a bias term.
- 2. Open loop validation of a turbine model using the (closed loop) measurement of the terminal voltage as a turbine model input may lead to errors due to a bias term caused by the feedback loop.
- 3. For the wind turbine model with grid impedance, the transfer function between terminal voltage and turbine current equals the inverse of the grid impedance. Therefore it is not possible to estimate the open loop wind turbine transfer function from the voltage at the turbine terminal to the turbine current.
- 4. The previous observations are equivalent to the observation that the wind speed and the voltage do not constitute independent variables but are correlated. The magnitude of this correlation in the relevant frequency domain should be checked before the voltage is used as an input in open loop validation.

A.2 Estimation of the correlation between wind speed and voltage

The previous section indicated that the use of the measured terminal voltage as input in model validation may lead to unacceptable errors. In this section, the parameters determining the error magnitude will be investigated for a specific case: validation of the model of the Alsvik wind farm. An indirect approach has to be taken, since it is not possible to quantify the effect of the feedback, i.e. the correlation between wind speed and terminal voltage, directly from the Alsvik measurements. The relevant wind speed is not known: a time delay of variable length exists between the (single point) measured wind speed at a meteo mast and the wind speed at the turbine rotor. Furthermore, the rotor effective wind speed is the relevant wind speed to be considered, since this is the driving 'force' of the turbine and the primary input signal of the model. To determine the rotor effective wind speed, additional measurements are required.

Therefore, the estimation of the correlation between wind speed and voltage will fully rely on modelling. The rationale is as follows: under representative system conditions (turbine and grid model and parameters) a simulation can be used to estimate the magnitude of the correlation between effective wind speed and terminal voltage. By quantifying the correlation between simulated wind speed and simulated voltage in the frequency domain relevant in the

validation, the error produced by using the voltage as input can be estimated. If the coherence function of rotor effective wind speed and voltage is sufficiently low over the relevant frequency range, the use of the measured voltage as an input in the model validation is acceptable. If the coherence over (part of) the range is high, the use of the measured voltage as an input should be discouraged.

As representative system conditions are chosen:

- the Alsvik wind farm (4 wind turbines, total rated power 0.72 MW) including turbine transformers and cables. Wind turbines are not operating in synchronism (different rotor positions, synchronisation is an exceptional condition);
- a grid model consisting of a controlled synchronous generator of 202 MW, overhead lines, transformers and loads of 110 MW in total;
- a short circuit ratio at the low voltage side of turbine transformer of 4.1 MVA, so about 23 times the rated power of a single turbine. This is a bit low, 50 times is standard, so it represents a relatively weak grid at the turbine.

The relatively weak grid configuration will give sufficiently large voltage variations to include most wind farms conditions. Then, the coherence between wind speed and voltage is expected to be relatively large. Two cases will be compared: with and without voltage variations induced by load changes in the grid.

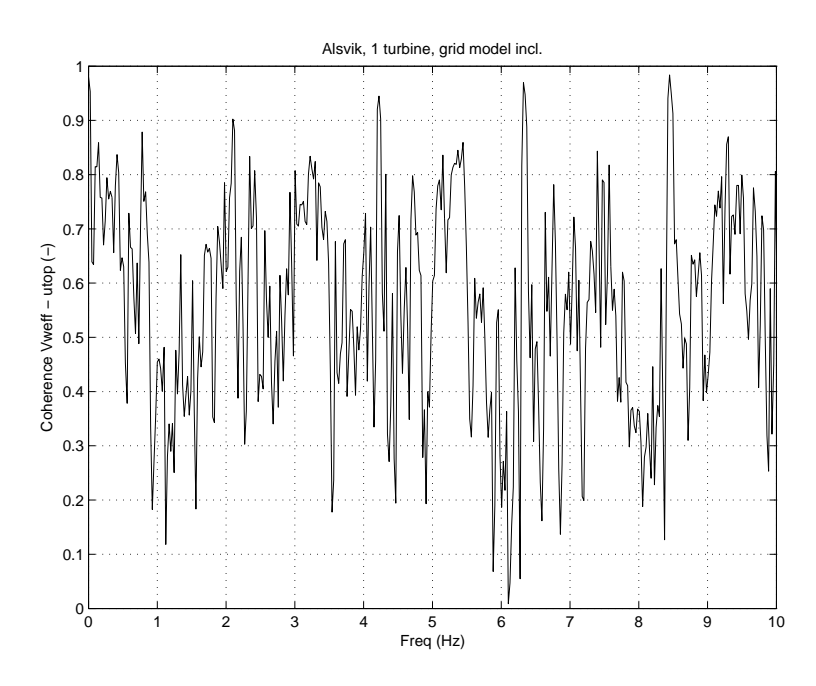


Figure 46: Coherence between rotor effective wind speed and terminal voltage for a single Alsvik turbine in operation, no grid load variations (simulation)

Figure 46 gives the coherence between the rotor effective wind speed and the terminal voltage for a single Alsvik turbine in operation. The figure shows a high coherence at multiples of 3P (0.90-0.98) and a relatively high coherence over the full range of 1-10 Hz (0.55 on average). This is not in favour of using the voltage as an input. It should be noted that this is typical for a constant speed turbine, where a strong link between wind speed variations and power variations exists. For a variable speed system, the coherence is expected to be much lower.

The coherence should reduce if the number of turbines in operation is increased and also if uncorrelated voltage variations caused by load changes in the grid are taken into account.

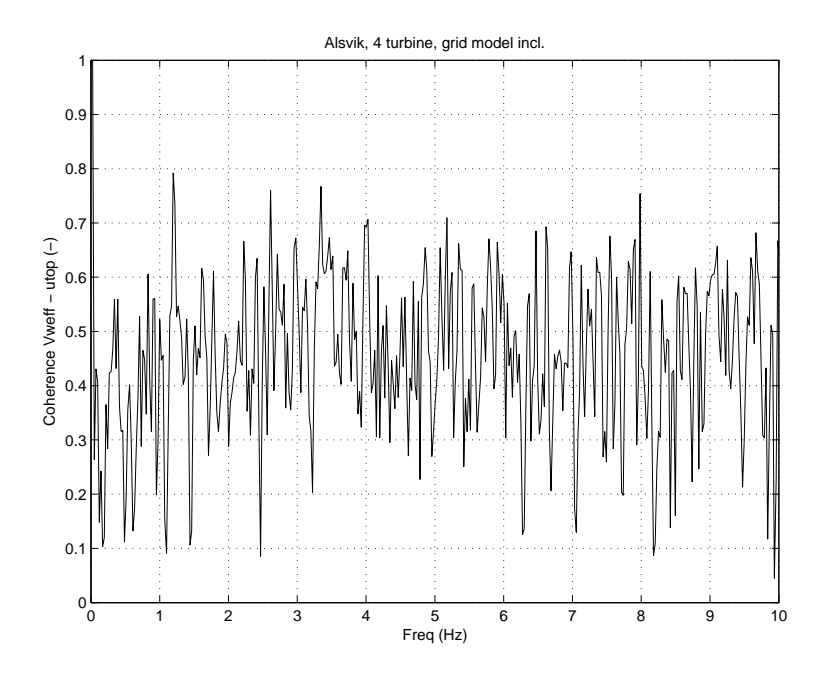


Figure 47: Coherence between rotor effective wind speed and terminal voltage for 4 Alsvik turbines in operation, no grid load variations (simulation)

Figure 47 gives the coherence between the rotor effective wind speed and the terminal voltage for a group of 4 Alsvik turbines in operation. Since the rotor positions are not synchronised, the rotationally sampled wind speeds of the different turbines are not strongly correlated and this reduces the correlation between the wind speed of a single turbine and the terminal voltage. However, the average coherence of 0.45 is still relatively high.

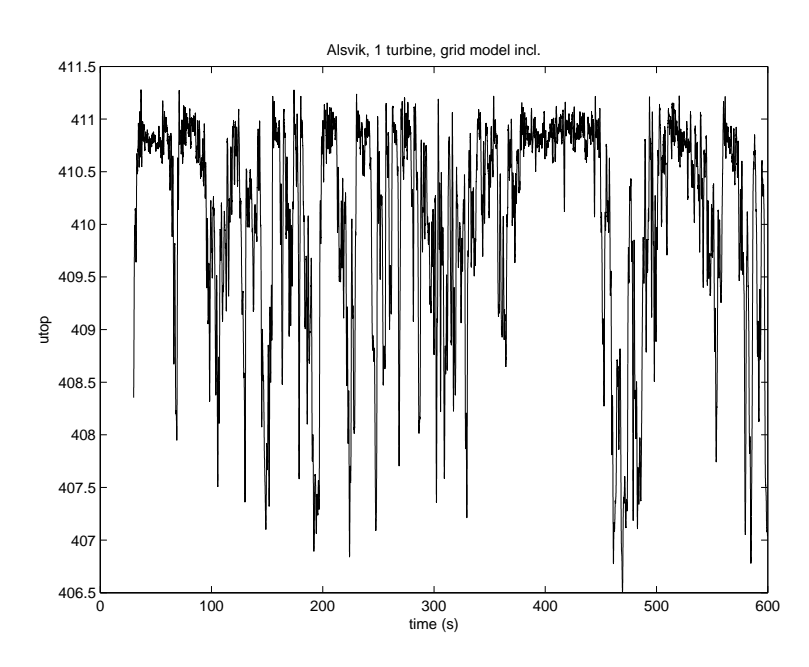


Figure 48: Terminal voltage variations for a single Alsvik turbine in operation (no grid load variations, simulation)

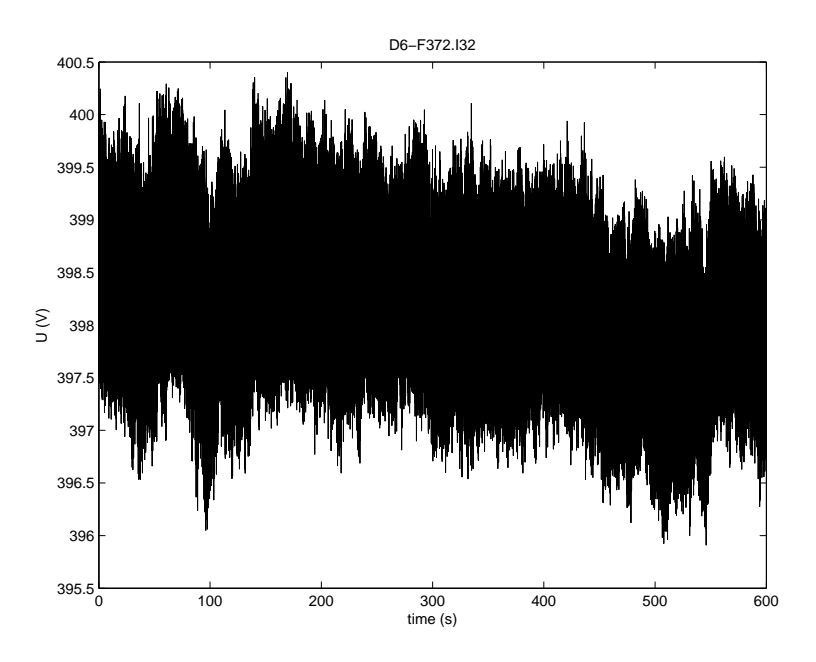


Figure 49: Terminal voltage variations for a single Alsvik turbine in operation (measured)

Figures 48 and 49 give the simulated and the measured terminal voltage of an Alsvik turbine. The absolute variation (ca. 3 V) is about equal. The measured voltage displays more variation and this noise is probably caused by load changes in the grid. Since these variations are independent of wind speed changes, including load variations in the simulation will reduce the coherence and have a positive effect on the prospect of using of the terminal voltage as an input variable. The effect will be estimated by introducing a random load change in the simulation with 1 Alsvik turbine in operation.

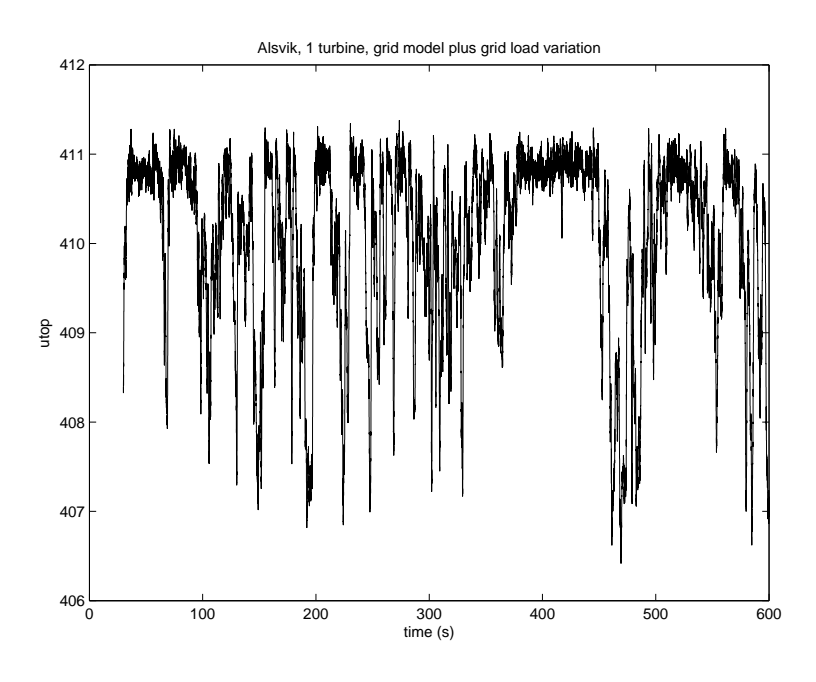


Figure 50: Terminal voltage variations for an Alsvik turbines during small grid load variations (simulation)

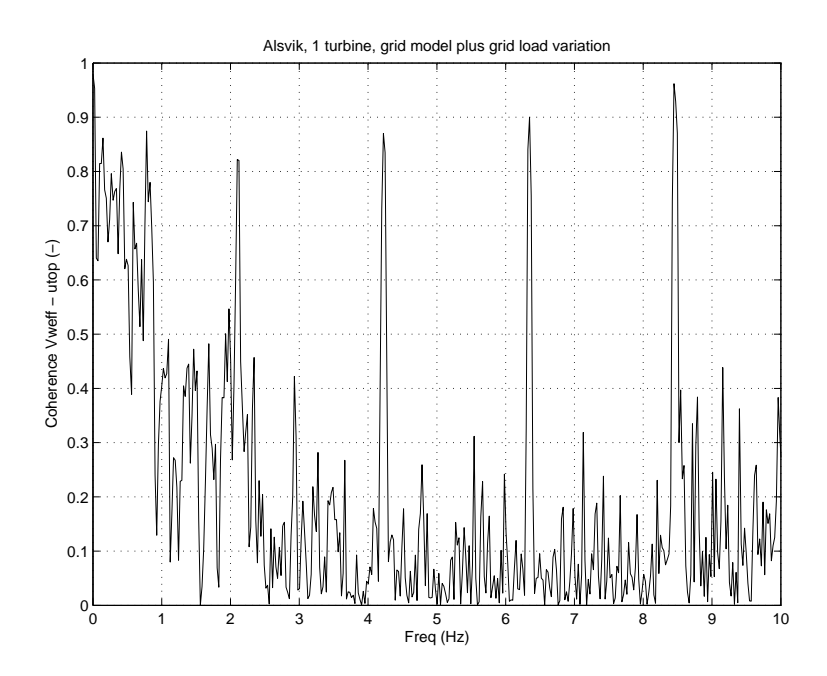


Figure 51: Coherence between rotor effective wind speed and terminal voltage for an Alsvik turbine including grid load variations causing 0.25 V voltage noise (simulation)

Two load variation magnitudes are investigated. In the first case, the load variation only has a small effect on the voltage variation, typically 0.25 V, see figure 50 and 51. The independent variations reduce the coherence between wind speed and voltage primarily in the region between the multiples of 3P. The effect at the n3P frequencies is small.

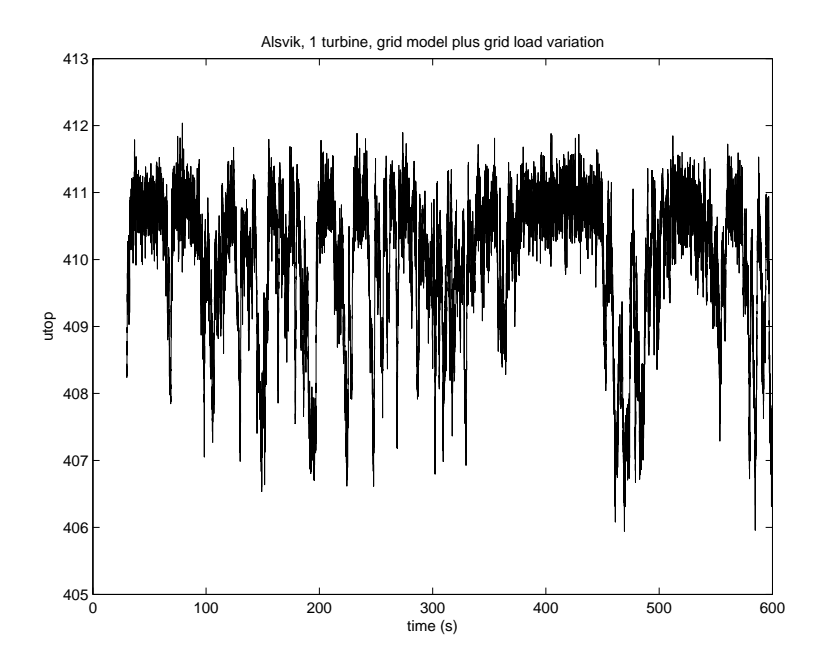


Figure 52: Terminal voltage variations for an Alsvik turbines medium grid load variations (simulation)

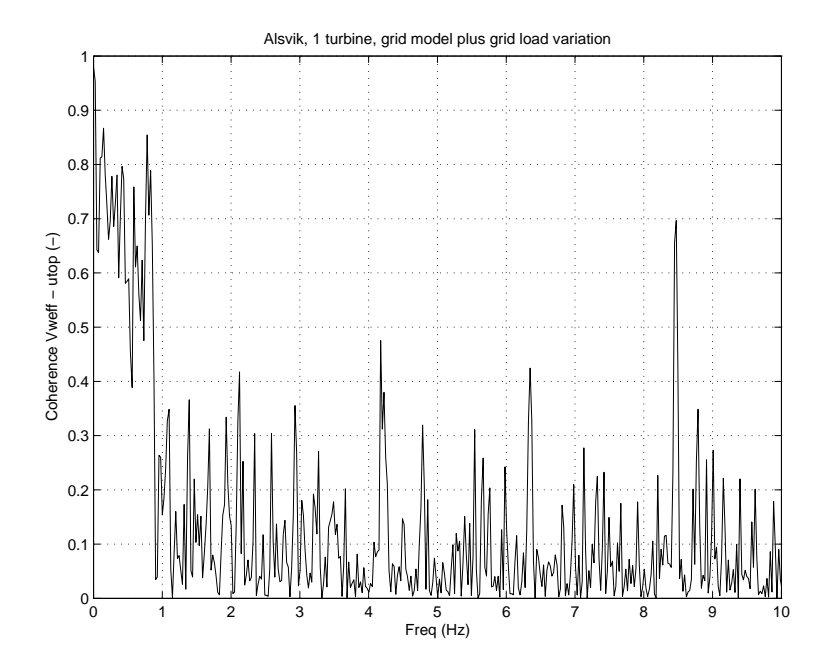


Figure 53: Coherence between rotor effective wind speed and terminal voltage for an Alsvik turbine including grid load variations causing 1 V voltage noise (simulation)

In the second case, the load variation is larger, resulting in voltage variations of 1 V, see figure 52 and 53. These voltage variations still are significantly smaller than the variations in the Alsvik measurements: about 3 V. The reduction of the n3P frequencies now is more substancial.

Conclusion

For the Alsvik wind farm was shown that multiple turbines in operation and a substancial amount of noise in the terminal voltage caused by load changes in the grid significantly reduce the correlation between the wind speed and the terminal voltage. Therefore it is permissible to use the measured (closed loop) voltage of the Alsvik wind farm to calculate APSD functions of currents and powers in the open loop model validation. This method will introduce an error, due to the coherence of the measured voltage and the rotor effective wind speed, which is not correctly represented in the open loop model validation. Since the coherence is relatively low, the error is expected to be small. As demonstrated in section A.1 it is not possible to use the measured terminal voltage to estimate the open loop transfer function between the voltage and turbine power or turbine current.

A.3 Summary of parameters in random processes

Since frequent use is made of parameters and variables that describe random processes, the definitions used in the analysis of random variables are summarised. For a more complete overview is referred to [4].

- (1) The probability that a variable x(t) is in the range between x and x + dx equals p(x)dx. The function p(x) is called the probability density function.
- (2) The probability distribution function P(x) is defined by $P(x) = \int_{-\infty}^{x} p(x) dx$.
- (3) The joint probability p(x,y)dxdy is the probability that x(t) is in the range between x and x+dx and at the same time y(t) is in the range between y and y+dy. For a finite interval: $\operatorname{Prob}(x_1 \leq x(t) \leq x_2)$ and $\operatorname{Prob}(y_1 \leq y(t) \leq y_2)$ equals $\int_{x_1}^{x_2} \int_{y_1}^{y_2} p(x,y) dx dy$. If x and y are independent, p(x,y) = p(x)p(y). The units of p(x,y) are 1/units of xy.
- (4) The average or mean value is the statistical expectation E of a random variable and is defined by: $E(x(t)) = \int_{-\infty}^{+\infty} x p(x) dx$. The units of E(x) are the units of x.
- (5) The average value of the square of a random signal thus equals: $E(x^2(t)) = \int_{-\infty}^{+\infty} x^2 p(x) dx$.
- (6) The standard deviation σ and the variance σ^2 follow from: $\sigma^2 = E[(x E[x])^2] = E[x^2] (E[x])^2$. The units of σ are the units of x.
- (7) For a function f(x,y) of two random variables x(t) and y(t), the average value of the function is defined through the joint probability p(x,y) of x and y:

$$E[f(x,y)] = \int_{-\infty}^{+\infty} \int_{-\infty}^{+\infty} f(x,y)p(x,y)dxdy.$$

(8) The joint expectation of two stochastic variables thus is:

$$E[x(t), y(t)] = \int_{-\infty}^{+\infty} \int_{-\infty}^{+\infty} xyp(x, y) dxdy.$$

- (9) The correlation coefficient or normalised covariance ρ_{xy} of two random variables x and y is defined by: $\rho_{xy} = \frac{E[(x-m_x)(y-m_y)]}{\sigma_x\sigma_y}$ with m_x, m_y the mean values of x and y.
- (10) The auto-correlation function $R_{xx}(\tau)$ is the average value of the product $x(t)x(t+\tau)$, i.e. $E[x(t)x(t+\tau)] = \int_{-\infty}^{+\infty} \int_{-\infty}^{+\infty} x(t)x(t+\tau)p(x(t)x(t+\tau))dx(t)dx(t+\tau)$. The units of R_{xx} are the units of x^2 .
- (11) The correlation coefficient ρ_{xx} of $x(t)x(t+\tau)$ and the autocorrelation function are related: $\rho_{xx}(\tau) = \frac{R_{xx}(\tau) m_x^2}{\sigma_x^2}$.
- (12) The cross-correlation function $R_{xy}(\tau)$ is the average value of the product $x(t)y(t+\tau)$, i.e. $E[x(t)y(t+\tau)]$. For a stationairy process, $R_{xy}(\tau) = R_{xy}(-\tau)$ but in general $R_{xy}(\tau) \neq R_{yx}(\tau)$.
- (13) Fourier transform in complex notation equals: $X(\omega) = \frac{1}{2\pi} \int_{-\infty}^{\infty} x(t) \mathrm{e}^{-j\omega t} dt$ and $x(t) = \int_{-\infty}^{\infty} X(\omega) \mathrm{e}^{j\omega t} d\omega$
- (14) The auto power spectral density function $S_{xx}(\omega)$ is the Fourier transformation of the autocorrelation function $R_{xx}(\tau)$: $S_{xx}(\omega) = \frac{1}{2\pi} \int_{-\infty}^{\infty} R_{xx}(\tau) \mathrm{e}^{-j\omega\tau} d\tau$. This is the two-sided version. Inverse transformation thus yields: $R_{xx}(t) = \int_{-\infty}^{\infty} S_{xx}(\omega) \mathrm{e}^{j\omega\tau} d\omega$. The units of S_{xx} are units of S_{xx} are unit of angular frequency.
- (15) Since $R_{xx}(\tau=0)=\int_{-\infty}^{\infty}S_{xx}(\omega)d\omega$ and $R_{xx}(\tau=0)=E[x^2]$, the area under the auto power spectral density function equals the mean square value of x. Therefore, a more complete name of $S_{xx}(\omega)$ is the mean square spectral density.
- (16) Similarly, the cross power spectral density function $S_{xy}(\omega)$ is the Fourier transformation of the cross correlation function $R_{xy}(\tau)$: $S_{xy}(\omega) = \frac{1}{2\pi} \int_{-\infty}^{\infty} R_{xy}(\tau) \mathrm{e}^{-j\omega\tau} d\tau$.

Frequency response of linear passive systems:

- (17) For input x(t) the output y(t) can be calculated in the frequency domain: $Y(\omega) = H(\omega)X(\omega)$, with $X(\omega) = \frac{1}{2\pi} \int_{-\infty}^{\infty} x(t) \mathrm{e}^{-j\omega t} dt = \mathcal{F}(x(t))$ and $H(\omega)$ the transfer function of the process.
- (18) In the time domain, the same result is obtained by the convolution integral which is based on the superposition principle applied to a linear system: $y(t) = \int_{-\infty}^{t} h(t-\tau)x(\tau)d\tau$, with h(t) the response of the process at time t to an impulse input at time 0.
- (19) Process response in terms of spectral density: $S_{yy}(\omega) = \sum_{r=1}^{N} \sum_{s=1}^{N} H_r^*(\omega) H_s(\omega) S_{x_r x_s}(\omega)$ with $x_{1,\dots,N}$ the input signals and $H_{1,\dots,N}(\omega)$ the transfer functions for a specific input.
- (20) For a single input: $S_{yy}(\omega) = H^*(\omega)H(\omega)S_{xx}(\omega) = |H(\omega)|^2S_{xx}(\omega)$.
- (21) For uncorrelated inputs: $S_{yy}(\omega) = \sum_{r=1}^{N} |H_r(\omega)|^2 S_{x_r x_r}(\omega)$.
- (22) Cross-correlation between output and an input for a system with multiple inputs. In case of two inputs: $R_{x_1y}(\tau) = \int_{-\infty}^{\infty} h_1(\theta) R_{x_1x_1}(\tau-\theta) d\theta + \int_{-\infty}^{\infty} h_2(\theta) R_{x_1x_2}(\tau-\theta) d\theta$
- (23) By taking the Fourier transform, the cross-spectral desity results: $S_{x_1y}(\omega) = H_1(\omega)S_{x_1x_1}(\omega) + H_2(\omega)S_{x_1x_2}(\omega)$.
- (24) For uncorrelated inputs $S_{x_1y}(\omega) = H_1(\omega)S_{x_1x_1}(\omega)$ and $S_{yx_1}(\omega) = S_{x_1y}^*(\omega) = H_1^*(\omega)S_{x_1x_1}(\omega)$ since $S_{x_1x_1}(\omega)$ is always a real quantity.
- (25) The coherence function for a single input-single output system is: $\eta_{yx_1}^2(\omega) = \frac{H_1(\omega)S_{yx_1}(\omega)}{S_{yy}(\omega)}$. Since $H_1(\omega) = \frac{S_{x_1y}(\omega)}{S_{x_1x_1}(\omega)}$ this is equivalent to: $\eta_{yx_1}^2(\omega) = \frac{S_{x_1y}(\omega)S_{yx_1}(\omega)}{S_{x_1x_1}(\omega)S_{yy}(\omega)}$.
- (26) The complex spectra can be writen in terms of the real coherence γ and the phase θ : $\frac{S_{xy}(f)}{\sqrt{S_{xx}(f)S_{yy}(f)}} = \gamma_{xy} \mathrm{e}^{-j\theta_{xy}(f)}.$
- (27) The periodogram ³ of a sampled signal of finite length L is calculated as follows: $\hat{P}_{xx}(f) = \frac{|X_L(f)|^2}{f_s L}$ with f_s the sample frequency and $X_L(f) = \sum_{n=0}^{L-1} x_L(n) e^{-2\pi j f_n/f_s}$ the discrete FFT [3].
- (28) The cross spectral density function $S_{xy}(\omega) = \sum_{m=-\infty}^{\infty} R_{xy}(m) e^{-j\omega m}$ is calculated as the product of the FFT of signal x times the conjugate of the FFT of signal y.
- (29) The estimate of the transfer function from x to y is $\hat{H}(\omega) = \frac{\hat{S}_{xy}(\omega)}{\hat{S}_{yy}(\omega)}$.
- (30) The coherence function of two signals x and y is estimated by $\hat{\eta}_{xy}(\omega) = \frac{\hat{S}_{xy}(\omega)}{\sqrt{\hat{S}_{xx}(\omega)\hat{S}_{yy}(\omega)}}$.

³ indicates that the value is an estimation

A.4 Cross and auto power spectral relation

With reference to figure 42 was stated that $S_{vw} = H_1 H_2^* S_{uu}$. This can be shown as follows:

$$v = H_1 u$$

$$w = H_2 u$$

$$S_{vw} = \int_{-\infty}^{\infty} e^{-j\omega\tau} E[v(t+\tau)w(t)]d\tau$$

$$v(t+\tau) = h_1(t+\tau) \cdot u(t+\tau) = \int_{-\infty}^{\infty} e^{j\omega(t+\tau)} H_1(\omega) dZ_u(\omega)$$

with $\int_{-\infty}^{\infty} e^{j\omega(t+\tau)} dZ_u(\omega)$ the spectral representation of $u(t+\tau)$, see Priestly. Similar:

$$w(t) = h_2(t) \cdot u(t) = \int_{-\infty}^{\infty} e^{j\omega't} H_2(\omega') dZ_u(\omega')$$

w(t) is a real process, so $w^*(t)=w(t)$ and $w^*(t)=\int_{-\infty}^{\infty}e^{j\omega't}H_2^*(\omega')dZ_u^*(\omega')$. Substituting:

$$S_{vw}(\omega) = \int_{-\infty}^{\infty} e^{-j\omega\tau} \{ \int_{-\infty}^{\infty} e^{j\omega(t+\tau)} \int_{-\infty}^{\infty} e^{-j\omega't} H_1(\omega) E[dZ_u(\omega)dZ_u^*(\omega')] H_2^*(\omega') \} d\tau$$

Now $E[dZ_u(\omega)dZ_u^*(\omega')] = S_{uu}(\omega)\delta(\omega - \omega')d\omega d\omega'$ with δ the Dirac function. So,

$$S_{vw} = \int_{-\infty}^{\infty} e^{-j\omega\tau} \{ \int_{\omega} \int_{\omega'} e^{j\omega(t+\tau)} e^{-j\omega't} H_1(\omega) S_{uu}(\omega) \delta(\omega - \omega') H_2^*(\omega') d\omega d\omega' \} d\tau$$

$$= \int_{-\infty}^{\infty} e^{-j\omega\tau} \{ \int_{\omega} e^{j\omega\tau} H_1(\omega) H_2^*(\omega) S_{uu}(\omega) d\omega \} d\tau$$

$$= H_1 H_2^* S_{uu}$$

B ALSVIK WINDFARM PARAMETERS

The Alsvik wind farm parameters used in the validation are listed in the next sections. The parameters have been supplied by Chalmers [12, 13] (TT) and Teknikgruppen [1] (IC). Some parameters have been estimated (JP). Some of the input parameters are not required in this context (indicated in the list by - -).

64 ECN-E-07-007

Table 10: Alsvik model parameters

Automatically generated parameter list from structcssAlsv.mat Turbine struct:

Variable	Description	Value	Source
	*		or N.R.
dLb	fi ne-mesh stepsize for tip speed ratio	0.10	
dTh	fi ne-mesh stepsize for pitch angle	0.10	
ThTbMin	minimum pitch angle value in aero data tables	-0.10	
ThTbMax	maximum pitch angle value in aero data tables	0.10	
CpTb	Cp table	matrix	TT, IC
CtTb	Ct table	matrix	TT, IC
CqTb	Cq table	matrix	TT, IC
LbTb	tip speed ratio	vector	TT, IC
ThTb	pitch angle	vector	TT, IC
nLb	number of tip speed values	20.00	
nTh	number of pitch angle values	1.00	
CprTb	resampled Cp table	matrix	
CtrTb	resampled Ct table	matrix	
CqrTb	resampled Cq table	matrix	
Lbr	resampled tip speed ratio	vector	
Thr	resampled pitch angle	vector	
nLbr	number of tip speed values resampled	96.00	
nThr	number of pitch angle values resampled	1.00	
ThMin	minimum pitch angle	-0.10	
ThMax	maximum pitch angle	-0.10	
LbMin	minimum tip speed ratio	3.00	
LbMax	maximum tip speed ratio	12.50	
Rb	rotor blade radius [m]	11.60	TT, IC
В	number of blades [-]	3.00	TT, IC
alphac	turbine blades cone angle [dg]	0.00	TT, IC
ThmaxWTB	cam fors turbine blades maximum vane and stall position	-0.10	
ThminWTB	cam fors turbine blades maximum vane and stall position	-0.10	
w0pt	typcial bandwitch pitch-actuator in speed servo mode [rad/s]	0.00	
betapt	typical damping rate pitch-actuator in speed servo mode [-]	0.03	
betat	damping rate of 1st tower bending mode [-]	0.0050	estm.
mt	tower top equiv. mass [kg]	9700	TT, IC
ct	tower top equiv. stiffness const. 1st bending mode [N/m]	497670	TT, IC
kt	tower top equiv. damper const. 1st bending mode [N/(m/s)]	694.79	calc.
w0t	natural frequency of 1st tower bending mode [rad/s]	7.16	TT, IC
Zt	tower height [m]	30.00	TT, IC
dtow	tower diameter	1.00	TT, IC
dn	rotor to tower distance for tower stagnation [m]	0.50	TT, IC
alphan	tilt angle of nacelle [dg]	5.00	TT, IC
rho	air density [kgm3]	1.23	JP
I15class	turbulence intensity at 15 m/s hub wind speed	0.18	JP
aclass	parameter for wind speed dependency of turbulence (2 for class IIA)	2.00	JP
LAMBDA1	turbulence length scale parameter [m] for more than 30m hubheight	21.00	JP
L1	integral scale parameter of longitudinal velocity component [m]	170.10	JP
alphashear	exponent in expression of windshear [-]	0.20	JP
Vcutin	cut-in average wind speed [m/s]	4.00	JP
Vcutout	cut-out wind speed [m/s]	18.00	JP
VwAnnual	annually average wind speed [m/s]	8.00	JP
UstairLo	stair-profi le windspeed start value [m/s]	9.00	

[H] [H]

Table 11: Alsvik model parameters (cont.)

Variable	Description	Value	Source
			or N.R.
UstairSzStep	step-size in stair profi le [m/s]	2.00	
UstairTmStep	duration of one step [s]	30.00	
UstairNrStep	number of steps in stair == nr. of different windspeeds minus 1 [-]	8.00	
Penom	nominal electric power [W]	180000	TT, IC
Wsyn	synchronic speed slow shaft [rad/s]	4.41	TT, IC
Rpmsyn	synchronic generator speed (fast shaft level) [rpm]	1000	TT, IC
snom	nominal generator slip [-]	0.01	TT, IC
Wnom	nominal speed slow shaft [rad/s] (electric power = Penom)	4.45	TT, IC
Tenom	nominal generator torque (slow shaft equiv) [Nm]	40419	TT, IC
iTran	gearbox transmission ratio [-]	23.75	TT, IC
Kam	gain in speed to torque transfer for 1st order model asynch. machine	916687	TT, IC
Tam	time-constant 1st order model asynchronous machine [s]	0.10	
Jr	moment of inertia turbine rotor [kgm2]	58098	TT, IC
Jg	moment of inertia generator [kgm2]	2538	TT, IC
w0hsd	1st torsion natural frequ. drive-train (fi xed slow shaft) [rad/s]	24.49	TT, IC
Betad	drive-train damping fraction of critical damping [-]	0.02	TT, IC
w0d	1st torsion natural frequ. drive-train + rotor [rad/s]	25.02	TT, IC
Je	equiv. mom. of iner. in equation of motion for shaft torsion [kgm2]	2432.03	TT, IC
cdr	drive-train stiffness [Nm/rad] (sl. sh. level)	1522969	TT, IC
kdr	drive-train damping constant [Nm/(rad/s)] (sl. sh. level)	2434.39	TT, IC
C1	Coulomb constant drive train [Nm]	0	TT, IC
C2	Viscous loss constant drive train [Nm(rad/s)]	0	TT, IC
Etanom	overall effi ciency in nominal conditions [-]	0.95	TT, IC
hrhoa	multiplier for fast aero power calculation ([W/(m/s)3], =0.5*rho*pi*Rb2)	258.92	calc.
hrhoar	multiplier for fast aero torque calculation ([Nm/(m/s)2], = hrhoa*Rb)	3003.52	calc.
muW	multipliers for fast evaluation of drive-train torsion equation [-, -]	0.04	calc.
muG	multipliers for fast evaluation of drive-train torsion equation [-, -]	0.96	calc.
Panom	nominal aerodynamic power	189474	TT, IC
Tanom	nominal aerodynamic torque slow shaft equiv [Nm]	42546	TT, IC
Thfi x	pitch angle value for maximum aero-power always nearest to Panom	-0.10	
Vwnom	wind speed for nominal aerodynamic power (or max. nearest to aero power)	12.20	TT, IC
Lbnom	lambda in nominal conditions	4.20	TT, IC
Fanom	axial force in nominal conditions	27070	TT, IC

Table 12: Alsvik model parameters (cont.)

Wind struct:

Variable	Description	Value	Source
			or N.R.
Uhubv	average wind speed on hubheight for calc. wind speed varations [m/s]	12.20	TT, IC
vwturbm36	3p- (AND) 6p-mode of rotationally sampled wind speed history	vector	output
nvwtow	normalised wind speed variations by tower stagnation	vector	output
nvwshr	normalised wind speed variations by wind shear	vector	output
vwturbm0	Op-mode in rotor effective rotionally sampled wind speed history	vector	output
vwfi x	turbulent wind speed variaton history in fi xed position	vector	output
vwstair	Op-mode in rotor effective rotionally sampled wind speed history	vector	output
timebase	time-index with stepsize Tdelsimv [s]	vector	output
azimbase	azimuth-index with stepsize Tdelsimv*(f0v*2*pi) [rad]	vector	output
fMinv	minimum frequency in turbulent wind variation	0.00	JP
fMaxv	maximum frequency in turbulent wind variation	25.00	JP